University of Windsor

Scholarship at UWindsor

Electronic Theses and Dissertations

Theses, Dissertations, and Major Papers

1-1-1967

An experimental investigation of the hysteresis phenomenon and effects of gap on curved wall jet separation.

P. K. Arora
University of Windsor

Follow this and additional works at: https://scholar.uwindsor.ca/etd

AN EXPERIMENTAL INVESTIGATION OF THE
HYSTERESIS PHENOMENON AND
EFFECTS OF GAP ON CURVED
WALL JET SEPARATION

A THESIS

Submitted to the Faculty of Graduate Studies through
the Department of Mechanical Engineering in partial
Fulfillment of the Requirements for the Degree
of Master of Applied Science at the
University of Windsor.

by

P. K. Arora

M.E., The University of Roorkee, India, 1964.

Windsor, Ontario, Canada

1967

UMI Number: EC52645

INFORMATION TO USERS

The quality of this reproduction is dependent upon the quality of the copy submitted. Broken or indistinct print, colored or poor quality illustrations and photographs, print bleed-through, substandard margins, and improper alignment can adversely affect reproduction.

In the unlikely event that the author did not send a complete manuscript and there are missing pages, these will be noted. Also, if unauthorized copyright material had to be removed, a note will indicate the deletion.

UMI®

UMI Microform EC52645
Copyright 2008 by ProQuest LLC.
All rights reserved. This microform edition is protected against unauthorized copying under Title 17, United States Code.

ProQuest LLC
789 E. Eisenhower Parkway
PO Box 1346
Ann Arbor, MI 48106-1346

AAW4106

Approved by: &K. L. Duan.

A. A. Luick.

D. E. L. Maasland

168110

ABSTRACT

The hysteresis phenomenon and angular position of separation were studied in a two-dimensional curved wall jet with different initial gaps between nozzle exit and leading edge of the wall. Nine different nozzle-curved wall combinations were used.

With an increase in the gap parallel to the nozzle axis, the loci of positions of the jet attachment and detachment and the approximate free jet boundary came closer together and the jet deflection became less stable. The maximum allowable gap parallel to nozzle axis was proportional to wall radius.

An increase in gap reduced angular position of separation ($\theta_{sep.}$), the gap parallel to the nozzle axis having less effect than perpendicular gap. The angle of separation initially increased with the product of Reynolds number and ratio of jet slot width to wall radius and finally approached a constant value. Almost the same effect was observed with different gaps.

iii

ACKNOWLEDGEMENTS

TABLE OF CONTENTS

vi

NOTATION

t   Jet nozzle width (ft.).

R   Radius of a wall (ft.).

h   Distance between nozzle lip and leading edge of deflection surface, parallel to the axis of the nozzle (ft.). See Fig. 1.

$h_{max.}$ Maximum allowable value of h.

v   Distance between nozzle lip and leading edge of deflection surface, perpendicular to the axis of the nozzle (ft.). See Fig. 1.

v_D , v_A Value of "v" at detached and attached position respectively.

m   Difference between v_D and v_A at a given "h".

Pa   Atmospheric pressure $(lbs./ft.^2)$.

Ps   Static pressure on the wall $(lbs./ft.^2)$.

P_T Total pressure in the jet at the nozzle exit $(lbs./ft.^2)$.

ρ Density of the fluid $(slugs/ft.^3)$.

ν Kinematic viscosity $(ft.^2/sec.)$.

θ   Angular position measured from the leading edge (degrees).

θsep.   Angular position of separation.

Re   Reynolds number $= \left[\dfrac{(P_T - P_a)\, Rt}{\rho\, \nu^2} \right]^{1/2}$.

Cp   Pressure coefficient $= \dfrac{(P_a - P_s)R}{(P_T - P_a)t}$.

Note: Superscript prime denotes dimensionless value in terms of the jet slot width. For example, $v' = \dfrac{v}{t}$.

viii

LIST OF FIGURES

ix

CHAPTER I

INTRODUCTION

When a curved wall surface is placed such that a jet emerges tangential to it, it is seen that the jet flows along the curved surface. This phenomenon is known as 'Coanda Effect' or 'Coanda Jet Deflection'.

The nature of the jet flow is complex. Turbulent mixing is predominant in the major outer part of the flow. But near the wall surface, the viscous effects have to be accounted for. Newman(Ref.1)and Fekete(Ref.2)have done considerable work on jet flow over a cylinder without a gap between the nozzle and curved surface. Korbacher (Ref. 3) and Benner (Ref. 4) studied gap effects by measuring the force acting on, and the surface pressure distribution over, a quadrant surface.

Recently, Paranjpe (Ref. 5) investigated the effects of a gap on the velocity profile, position of jet separation, static pressure distribution and also studied the hysteresis phenomenon. He kept the nozzle width and wall radius constant. The present investigation studies the hysteresis phenomenon and gap effect on wall jet separation using different nozzle-curved wall combinations. The surrounding fluid was stationary and

1

the flow was in the incompressible range.

CHAPTER II

LITERATURE SURVEY

The material covered in this chapter summarizes briefly the existing literature and is included in the report for the sake of completeness and ease of reference. Jet flow over a curved wall without an initial gap is considered first in the following sections. A knowledge of this flow is necessary for our investigation.

2.1 IDEAL FLUID FLOW

The bending of a jet sheet is produced by a pressure difference acting across it. Considering an element in a two dimensional flow of a thin jet ($t \ll R$) of an ideal fluid and equating the centrifugal and the pressure forces which are in radial equilibrium, the pressure coefficient Cp is expressed as:

$$Cp = \frac{(Pa - Ps)R}{(P_T - Pa)t} = 2 \qquad (2.1)$$

The experimental results of Korbacher (Ref. 3) agree well with equation (2.1) for small values of θ. But the values obtained by Newman (Ref. 1) and Fekete (Ref. 2) are less than that predicted by equation (2.1).

2.2 REMARKS ON REAL JET FLOW

The real fluid jet continuously entrains fluid from the surroundings. Thus the jet width increases and the fluid velocity decreases with an increasing Θ. In consequence, the pressure at the surface which is initially lower than Pa due to the flow curvature, tends to approach Pa as the jet velocity decreases. Hence the entrainment of the surrounding fluid produces the pressure rise that finally causes the jet to separate from the surface. This emphasizes the necessity of including the process of entrainment in any theoretical analysis.

2.3 NEWMAN'S ANALYSIS (DIMENSIONAL APPROACH)

The following parameters are sufficient to define an incompressible jet flow over a curved surface:

$(Pa-Ps)$, (P_T-Pa), t, R, ν, ρ and Θ.

The pressure difference across the jet sheet $(Pa-Ps)$ at an angular position Θ, may therefore be related non-dimensionally to these parameters as follows:

$$\frac{(Pa-Ps)}{(P_T-Pa)} = f\left[\Theta, \frac{t}{R}, \left\{\frac{(P_T-Pa)R^2}{\rho \ \nu^2}\right\}^{1/2}\right] \qquad (2.2)$$

At some distance from the slot we might expect the flow to become independent of the separate parameters (P_T-Pa) and t and depend only on their product $(P_T-Pa) \cdot t$ as long as suitable zero is chosen for Θ. Furthermore, for large

values of Reynolds number the flow will tend to become

independent of viscosity so that

$$\frac{(P_a - P_s)R}{(P_T - P_a)t} = f(\theta) \qquad (2.3)$$

From equation (2.2), the angular position of separation

θsep. can be expressed as follows:

$$\theta\text{sep.} = f\left[\frac{t}{R}, \left\{\frac{(P_T - P_a)Rt}{\rho \, \nu^2}\right\}^{1/2}\right] \qquad (2.4)$$

If the position of separation is sufficiently far

from the slot, θsep. depends only on R_e,

$$\theta\text{sep.} = f\left[\left\{\frac{(P_T - P_a)Rt}{\rho \, \nu^2}\right\}^{1/2}\right] \qquad (2.5)$$

At large Reynolds number θsep. with suitably

chosen zero, tends to become constant. In particular, for

small values of t/R, θsep. measured from the slot is con-

stant. Experimental results (Ref. 1) confirm the above

statement and they show that for t/R values ranging from

0.02 to 0.04, θsep. = 240°.

2.4 GAP EFFECT

In 1962, Korbacher (Ref. 3) investigated gap

effect on a curved wall jet by measuring the forces and

pressure acting on a quadrant. He found that the coanda

phenomenon was also effective when the deflection surface

was separated from the nozzle by a wide gap open to the

atmospheric pressure. The experiments were carried out for
nozzle pressure ratios up to and well above the critical.
Gaps along the nozzle axis up to eight times the jet slot
width (at R = 2.5 in.) have practically no effect on the
component of the force in the direction normal to the
nozzle axis. Maximum v' (at any given h') for which the
jet was able to bridge the gap depended on the jet slot
width. The larger the t, the smaller is the v'. He con-
cluded that the effect of h' on the static pressure
distribution on the wall was small. These findings were
confirmed by Benner's investigation (Ref.4) which was a
continuation of the work reported by Korbacher.

Paranjpe (Ref. 5) recently studied the gap effects
on velocity profiles, position of separation and static
pressure distribution. With different gaps, he found that
in a region close to the leading edge of the wall, the
velocity profile and rate of jet growth and maximum velocity
decay were different from and eventually approached that of
no gap. The settling region where the type of flow changed
from a free jet to a wall jet, was found to increase with
the gap size. The flow in the outer layer was unaffected
by the gap. The pressure difference across the jet initially
increased with gap size but at larger angles, the pressure
difference reduced more rapidly for larger gaps indicating
earlier separation. The value of angular position of

separation ($\Theta_{sep.}$) decreased with an increase in gap size.

For a given h, the jet attached to and detached from the curved wall at different values of v, namely, v_A and v_D respectively. This is known as the hysteresis phenomenon. Paranjpe (Ref. 5) found that with an increase in h, the difference between v_A and v_D decreased and their values approached that of the approximate free jet boundary Korbacher (Ref. 3) also made a note of the hysteresis phenomenon.

CHAPTER III

TEST FACILITIES

The apparatus is shown in Figures 1, 2 and 3.
References to the letter code used in Fig. 1 are made in
the description of the test facilities.

3.1 AIR SUPPLY AND GUIDING DUCT

Air was supplied by a type HS, Size 200 American
Standard Centrifugal fan (A) with static pressure of 5 in.
of water. This fan was driven by a 5 h.p., 1745 r.p.m.
General Electric induction motor. A 30 in. long, wooden
guiding duct (B) with a rectangular cross section was
attached to the fan exit. A honeycomb flow straightener
was placed in the guiding duct to reduce the turbulence
level induced by the fan.

3.2 CONTRACTION DUCT AND NOZZLES

A wooden contraction duct (C) 30 in. long was
placed after the guiding duct. A converging nozzle (D) made
of brass was attached to the contraction duct. Nozzles used
were 0.25 in., 0.125 in. and 0.0625 in. wide and each had
9 in. span. The contraction ratios for the o.25 in. nozzle
together with the duct were 62:1 in the direction of 0.25 in.
width and 2.5:1 in the perpendicular direction.

3.3 WALLS AND TRAVERSING MECHANISM

Curved walls having radii 3 in., 6 in. and 9 in. and each consisting of a 9 in. long half cylinder made of smooth plexiglass were used.

A piece of 30 in. x 40 in x 0.25 in. plexiglass plate on the top and a combination of rolled steel plate and plexiglass plate at the bottom were used as end plates to obtain the two dimensional flow condition. The wall (E) was mounted perpendicular to the end plates with the 9 in. direction being parallel to the spanwise direction of the jet slot.

The mechanism used for moving the wall to the required gap position, was capable of moving the wall both parallel and perpendicular to the jet. In both the directions, distances could be measured to an accuracy of 0.005 inch.

The traversing mechanism was provided with levelling screws to ensure correct alignment with the nozzle exit.

3.4 PROBING EQUIPMENT

A flattened stainless steel hypodermic tube with an opening of 0.005 in. x 0.060 in. was used to measure the total pressure in the jet. The probe was mounted on a traversing mechanism which moved the probe with an accuracy of 0.001 inch. An inclined manometer with an accuracy of

0.001 in. of water was utilised for pressure measurements.

CHAPTER IV

EXPERIMENTS

For each nozzle, the two dimensionality of the jet flow was checked by probing the jet at different spanwise locations. No significant changes in the velocity distributions were noted.

Throughout the experiment, the jet velocity at the nozzle exit was kept constant (145 ft./sec.). The Reynolds number ranged from 2.256×10^4 to 7.781×10^4.

With each nozzle-curved wall combination, the hysteresis phenomenon and wall jet separation were investigated.

4.1 THE HYSTERESIS PHENOMENON

For any gap h', when the curved surface was moved away from the jet (v' increased), at a particular value of v' (say v'_D), the jet sheet detached from the surface. But when the curved surface was brought back (v' reduced), the jet did not attach to the surface at v'_D but attached at a lower value of v', namely, v'_A ($v'_A < v'_D$). This was because the jet had a tendency to maintain the detached or attached flow configuration until sufficiently affected by the movement of the curved surface. Further, both the attachment and detachment processes were rather abrupt in nature,

the detachment being somewhat less sudden than the attach-
ment. v'_D and v'_A were determined by keeping the total
pressure probe at a suitable distance from the nozzle and
curved wall. At different values of h', these "attached"
and "detached" positions were noted and "attached line"
and "detached line" were plotted. This information (Fig. 4)
was also useful for determining the range of gap sizes for
other experiments.

4.2 VISUALIZATION OF FLOW SEPARATION

In order to determine the angular position of
separation (θsep.), a well proportioned mixture of lamp
black and kerosene was applied to the curved surface of the
wall (Fig. 5). In the attached flow region, the motion of
lamp black particles was influenced by two factors, namely,
the jet flow and pull of gravity. In the region after
the flow separation, the lamp black particles were not
affected by the jet flow and hence the particle traces were
vertical (Fig. 6). Following the flow direction, the loca-
tion of the first vertical trace gave the position of jet
separation from the wall.

The values of θsep. were determined for the
curved wall jet with different values of v keeping h
constant. This was done for three or more different values
of h for each nozzle-curved wall combination.

CHAPTER V

EXPERIMENTAL RESULTS

5.1 THE HYSTERESIS PHENOMENON

Figures 4(a,b,c) show the variation of the "attached" and "detached" positions with h' for 0.0625 in., 0.125 in. and 0.25 in. nozzle respectively (R being the same) while Fig. 4(c,d,e) are respectively for 3 in., 6 in. and 9 in. curved wall (t being the same). The approximate free jet boundary is also shown in Fig. 4. It is seen that the difference between the values of v' for "detached" and "attached" positions, m', first decreases slowly and then rapidly as h' increases in all cases. It is interesting to note that the three lines come closer together as h' is increased.

Further, it was observed during the experiments that for large values of h', the deflection of the jet by means of the curved surface was not very stable. This may be explained by the fact that the value of m' was small. This indicates that for a given nozzle-curved wall combination there is a maximum allowable value of h' denoted by h'$_{max.}$. The h'$_{max.}$ as seen from Fig. 4 increases with a decrease in t (keeping R constant) and increases with an increase in R (keeping t constant). This is also shown in

Fig. 7. We see that $h'_{max.}$ is proportional to $\frac{R}{t}$. This relationship was also intuitively expected from the simple theory which predicts that $Cp = \frac{t}{R}$. Since $h'_{max.}$ is proportional to R', $h_{max.}$ is proportional to R.

It is seen that the results obtained with different combinations of R and t agree with those obtained by Paranjpe (Ref. 5) qualitatively.

Figure 8 shows the variation of v_D with $(Rt)^{1/2}$ for different h. It is seen that as $(Rt)^{1/2}$ increases, v_D also increases. At a given value of $(Rt)^{1/2}$, it is noted that v_D increases with a decrease in t or an increase in R. Further, it is seen that as t tends to zero, the constant t-plot tends to the ordinate. Also as R tends to zero, the constant R-plot tends to the origin. Thus for a wall of zero radius, v_D is zero. Hence the constant t-plots are extrapolated to pass through the origin. The constant R-line can be extrapolated to get the limiting value of t above which the jet will remain detached, i.e., $v_D = 0$.

Figure 9 is a dimensional plot between v_A and $(Rt)^{1/2}$. It is seen that this plot is similar in nature to that of Fig. 8. However, the effect of h on v_A is greater than that on v_D.

Plots in Fig. 10 show the "detached" positions for

different values of h' and R'. It is seen that v'_D increases
with R' and the dependance of v'_D on h' is very weak. Using
the statistical method of linear regression the best line to
fit the experimental data was drawn (correlation coefficient =
0.9932) and the following empirical relation was obtained:

$$v'_D = 0.061 \ (R')^{1.312}$$

For the "attached" positions, similar trends are
obtained as given in Fig. 11. However, in this case, the
effect of h' is more pronounced than the "detached" case.
The empirical relation could be expressed as:

$$v'_A = C(R')^n$$

where the values of the constants C and n depend on h' (see
Fig. 11 b).

5.2 SEPARATION

Had the curved surface been a full cylinder, separa-
tion would have been between 200° and 220°, for zero gap
and the Reynolds number range used (Ref. 2). But a half
cylinderical surface perhaps being more useful for practical
applications, was selected. For no gap, θsep. was between
125° and 175° depending on Re as shown in Fig. 12. It is
noted that θsep. initially increases with an increase in Re
but remains a constant at high Reynolds number. This is in
agreement in principle with Fekete's result (Ref. 2).
However, we notice a definite trend depending on R. An

improvement is obtained by plotting θsep. Vs. $\frac{Re}{R'}$ (Fig. 13).

Figure 14 shows θsep. Vs. v' for different h', t and R. It is seen that a gap reduces θsep., reduction becoming appreciable as v' tends to v'_D. It is evident that θsep. depends both on h' and v', larger the value of h' and v', smaller the angle θsep..

Further, when the curves in Fig. 14 are extrapolated to intercept the abscissa, the values of v' obtained are very close to the corresponding v'_D. This brings out the point that detachment is the limiting case of separation.

The effect of v' on the reduction of θsep. is more pronounced than that of h'. Therefore, in the following discussion of θsep. results, only the h' = 0 lines in the plots of Fig. 14 are considered.

Considering the rate of decrease of θsep. with v', we note that it increases with a decrease in R (t kept constant) and an in increase in t (R kept constant). This can be explained by the earlier detachment.

The variation of θsep. with $\frac{Re}{R'}$ for different $\frac{v}{v_D}$ is shown in Fig. 15. The experimental mean lines from Fig. 13 and Fig. 15 are shown together in Fig. 16 from which we see that even with different gaps, the effect of $\frac{Re}{R'}$ on θsep. is almost the same.

CHAPTER VI

CONCLUSIONS

6.1 THE HYSTERESIS PHENOMENON

1. With an increase in h', the "attached line", "detached line" and approximate free jet boundary come closer together and the jet deflection by means of a curved surface becomes less stable.

2. h_{max}. is proportional to R.

3. For any given radius, there is a limiting value of t above which the jet will remain detached.

4. v'_D or v'_A can be expressed as:

$$v'_D \text{ or } v'_A = C(R')^n$$

The constant "C" and index "n" do not change appreciably in the case of v'_D and the relation is:

$$v'_D = 0.061(R')^{1.312}.$$

6.2 SEPARATION

1. An increase in gap reduces $\Theta sep.$, reduction becoming appreciable as v' approaches v'_D.

2. v' has more effect on $\Theta sep.$ than h'.

3. The rate of decrease of $\Theta sep.$ with v' for constant h' increases with a decrease in R (t kept constant) and an increase in t (R kept constant).

4. A plot of $\Theta sep.$ Vs. $\frac{Re}{R'}$ is better than that of $\Theta sep.$ Vs. Re.

5. Θsep. initially increases with $\frac{Re}{R'}$ but remains a constant at high $\frac{Re}{R'}$.

6. Even with different gaps, the effect of $\frac{Re}{R'}$ on Θsep. is almost the same.

REFERENCES

1. Newman, B.G.　　The Deflection of Plane Jets by Adjacent Boundaries - Coanda Effect. Boundary Layer and Flow Control, Vol. 1, Edited by G.V.Lachman, Pergamon Press, P. 232, (1961)

2. Fekete, G.I.　　Coanda Flow of a Two Dimensional Wall Jet on the Outside of a Circular Cylinder. McGill University, Report No. 63 - 11. (1963)

3. Korbacher, G.K.　　The Coanda Effect at Deflection Surfaces Detached from the Jet Nozzle. Can. Aeronautics and Space Jnl., Vol. 8, No. 1, (Jan., 1962)

4. Benner,S.D.　　The Coanda Effect at Deflection Surfaces Widely Separated from the Jet Nozzle, UTIAS Technical Note No. 78, (April, 1965)

5. Paranjpe, S.C.　　An Experimental Investigation of the Effects of an Initial Gap on the Jet Flow over a Curved Wall, M.A.Sc. Thesis, Dept. of Mech. Engg., University of Windsor, Windsor, (1966)

19

AIR IN

TO MANOMETER

KIEL PROBE

A

B

C

D

E

G

H

MOTOR

A   FAN

B   GUIDING DUCT

C   CONTRACTION

D   NOZZLE

E   THE CURVED WALL

G   END PLATES

H   TOTAL PRESSURE PROBE
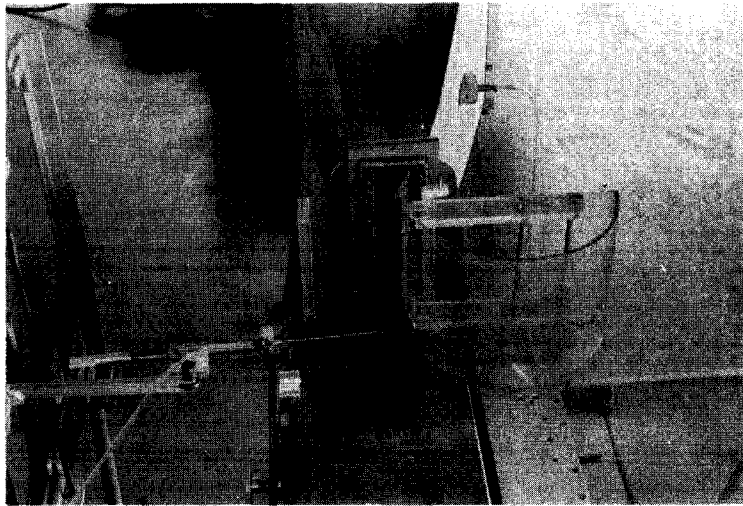
PROBING
MECHANISM

TO MANOMETER
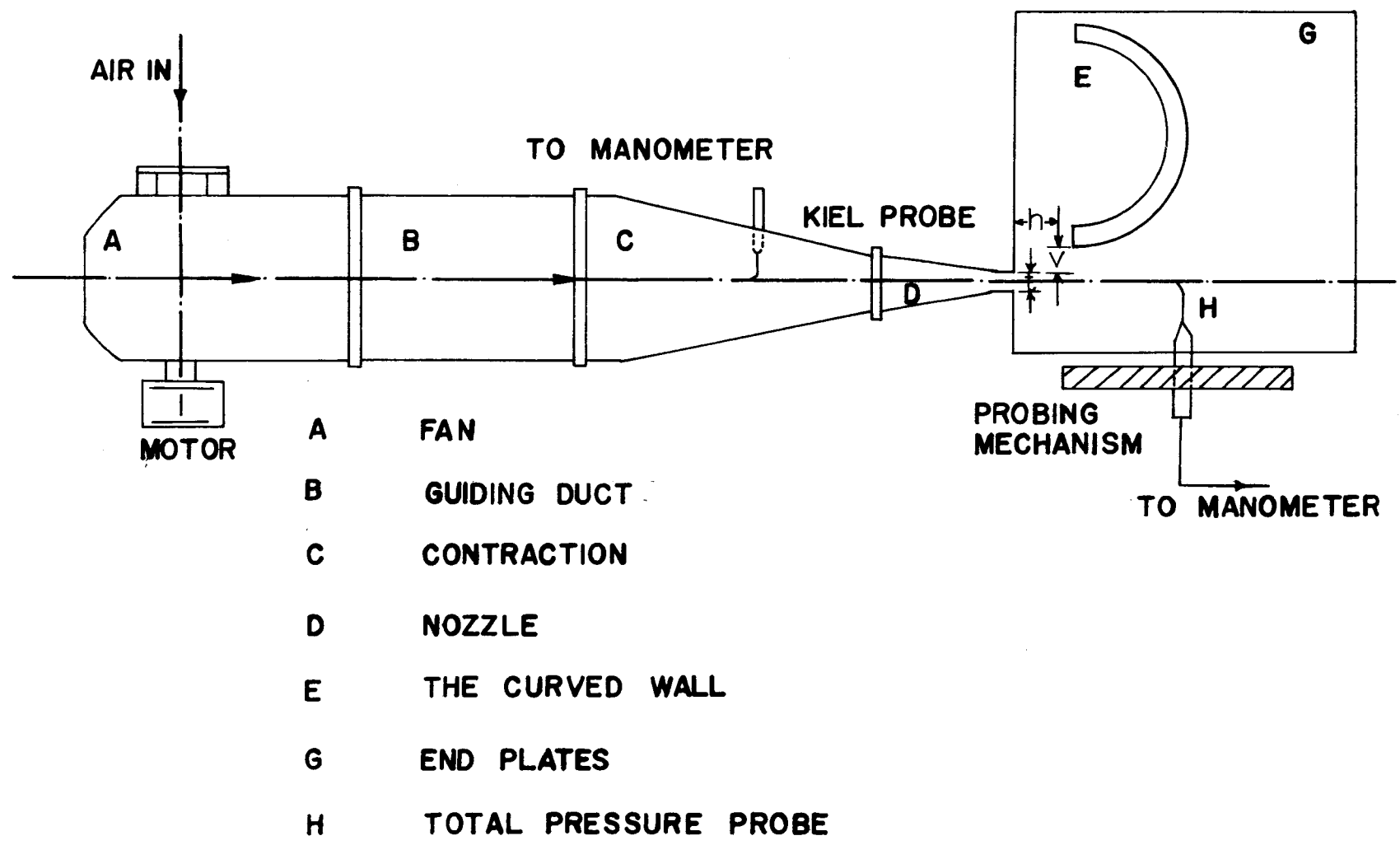
Fig. I SCHEMATIC DIAGRAM OF TEST FACILITIES
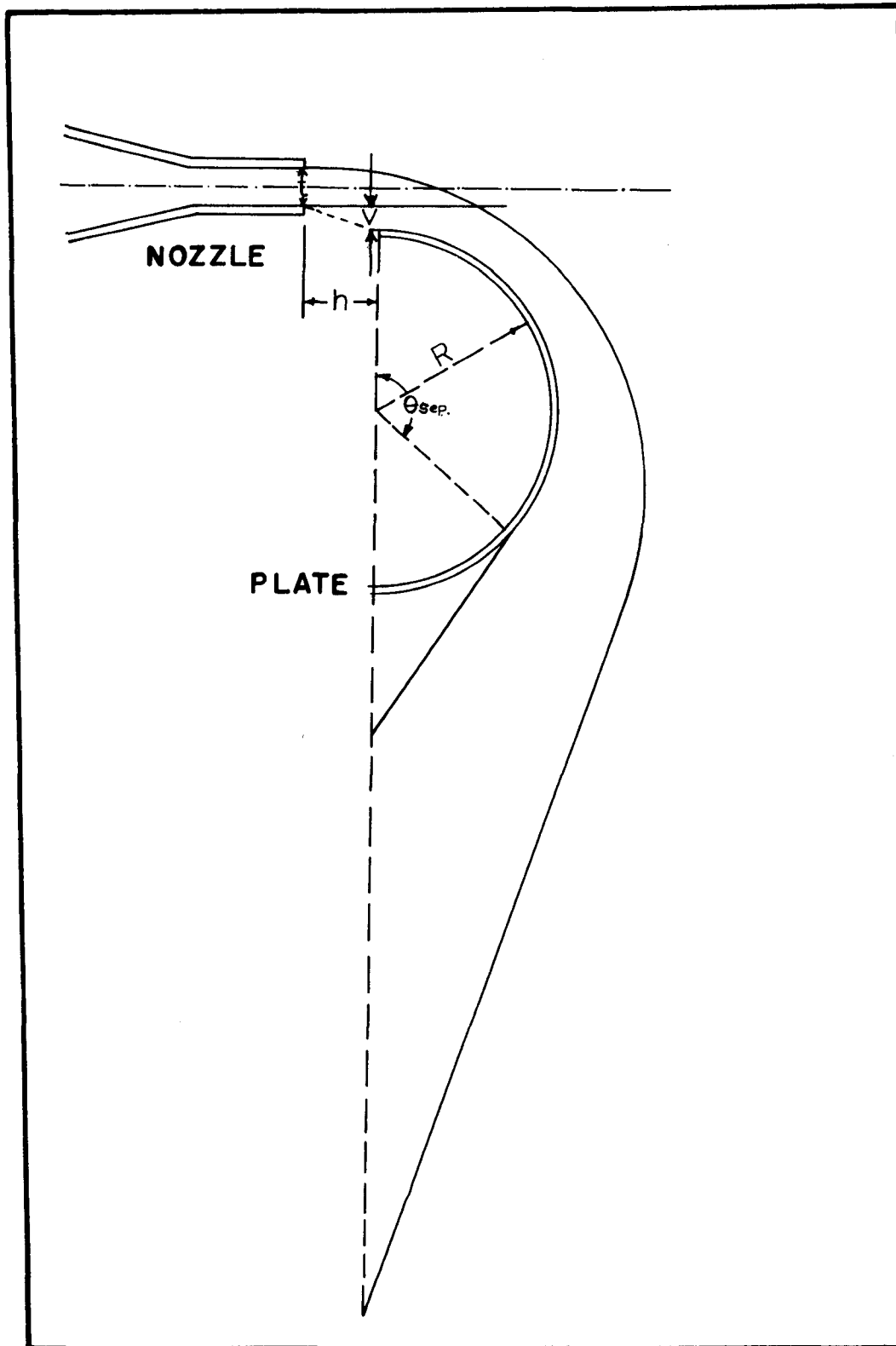
Fig. 2 SKETCH OF TEST REGION

Fig. 3   VIEW OF EXPERIMENTAL ARRANGEMENT
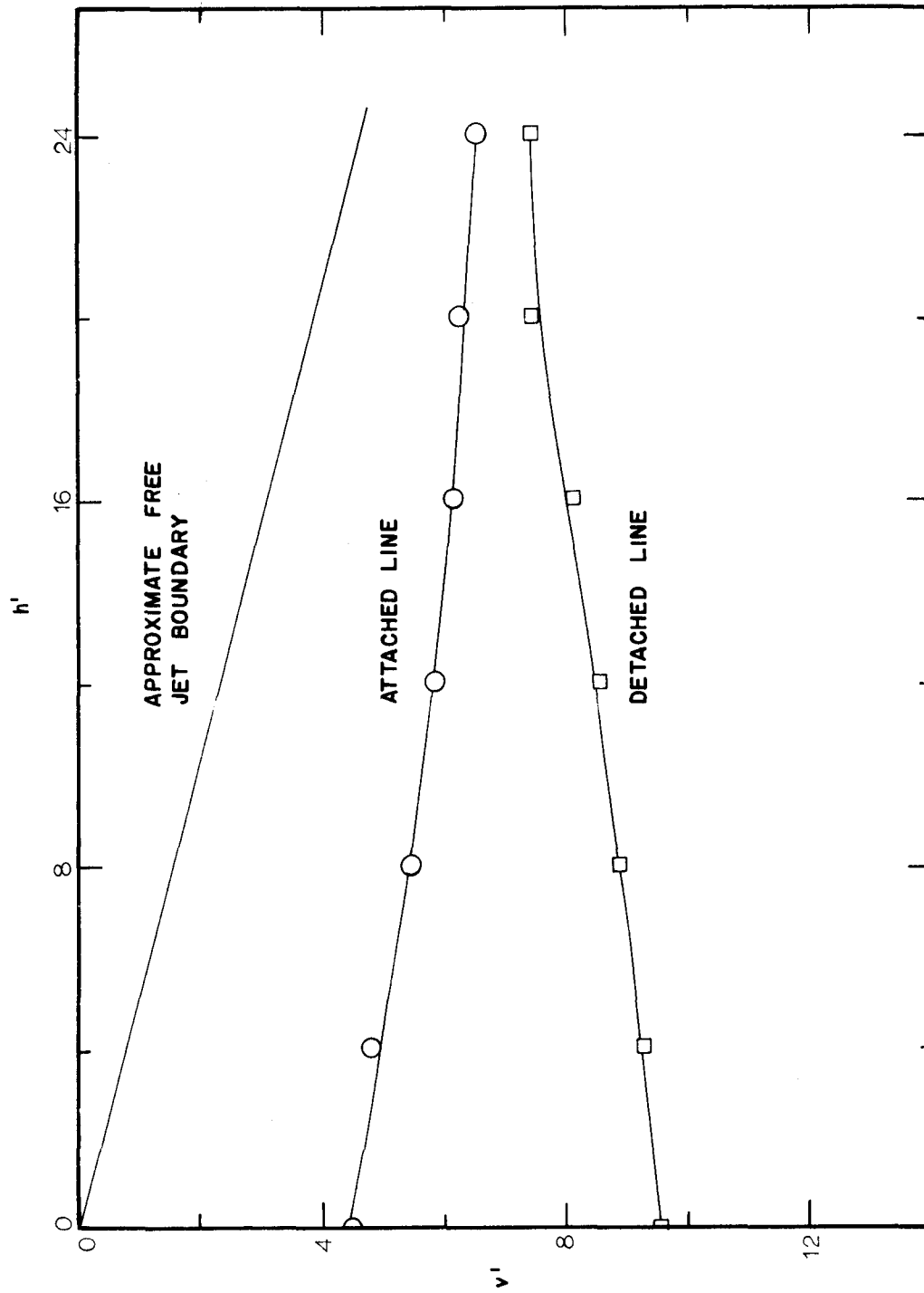
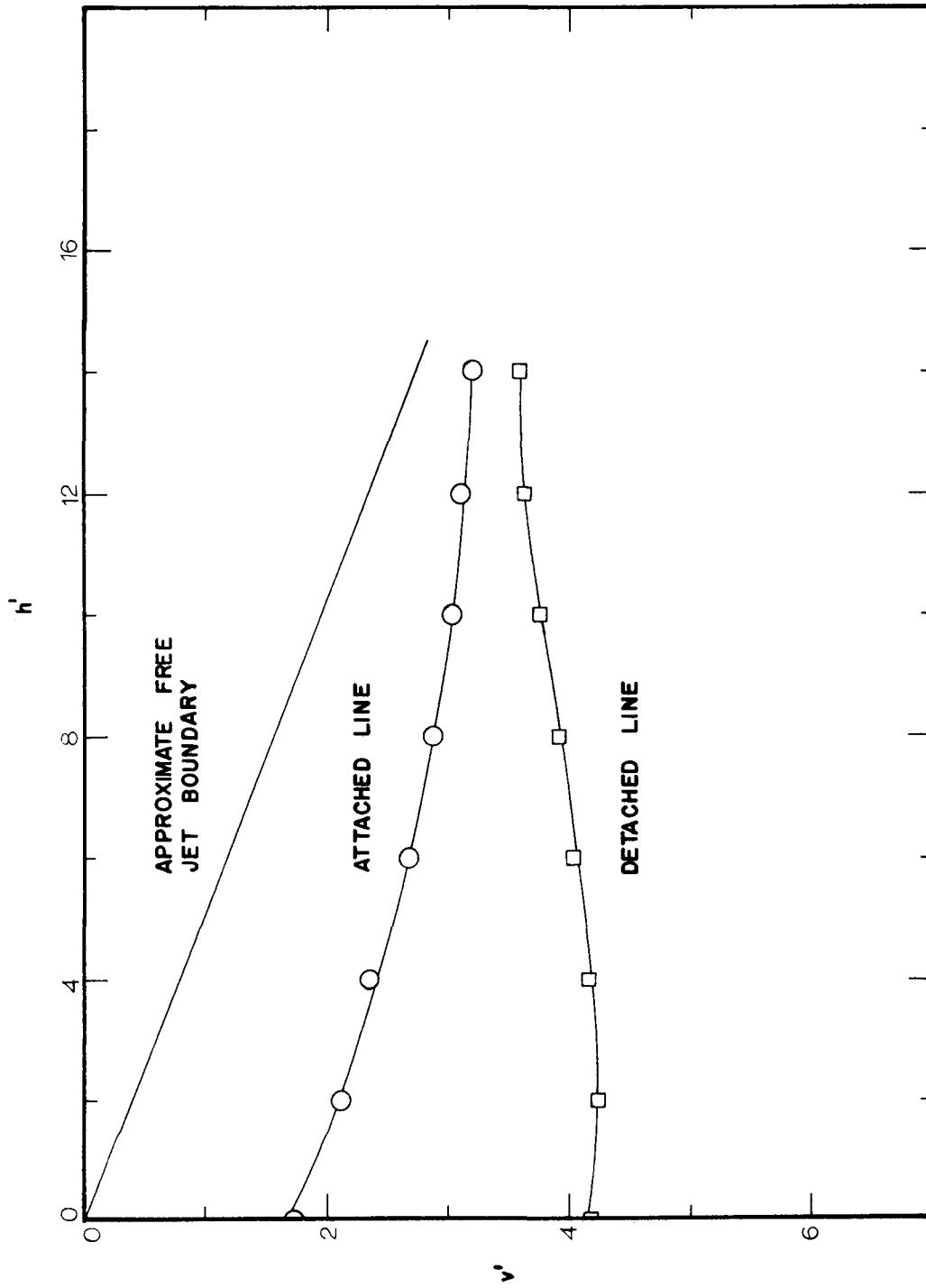Fig.4 a HYSTERESIS PLOT (R=3 in., t = 0.0625 in.

APPROXIMATE FREE
JET BOUNDARY

ATTACHED LINE

DETACHED LINE

h'

v'

Fig. 4b HYSTERESIS PLOT (R = 3 in., t = 0.125 in.)
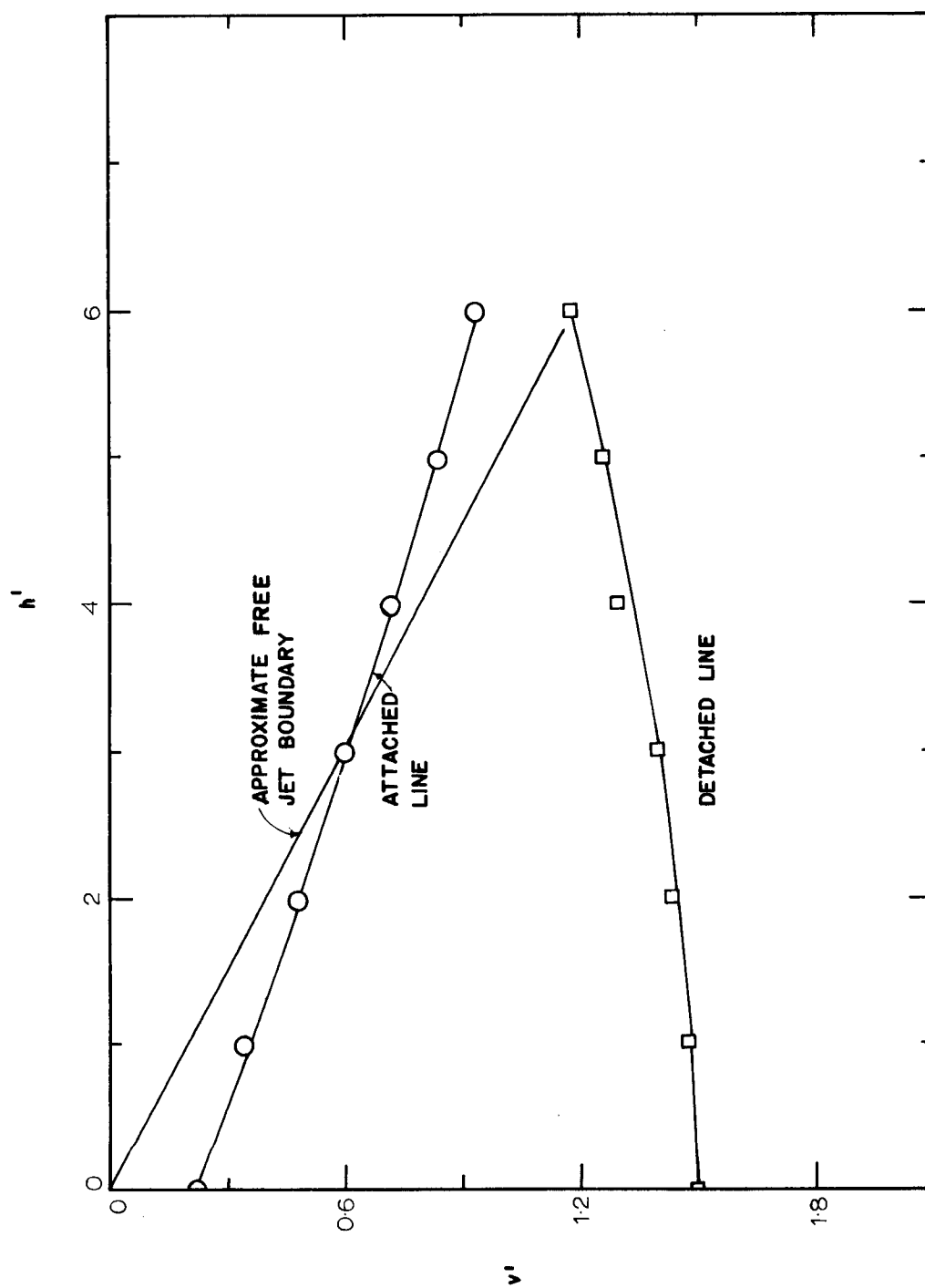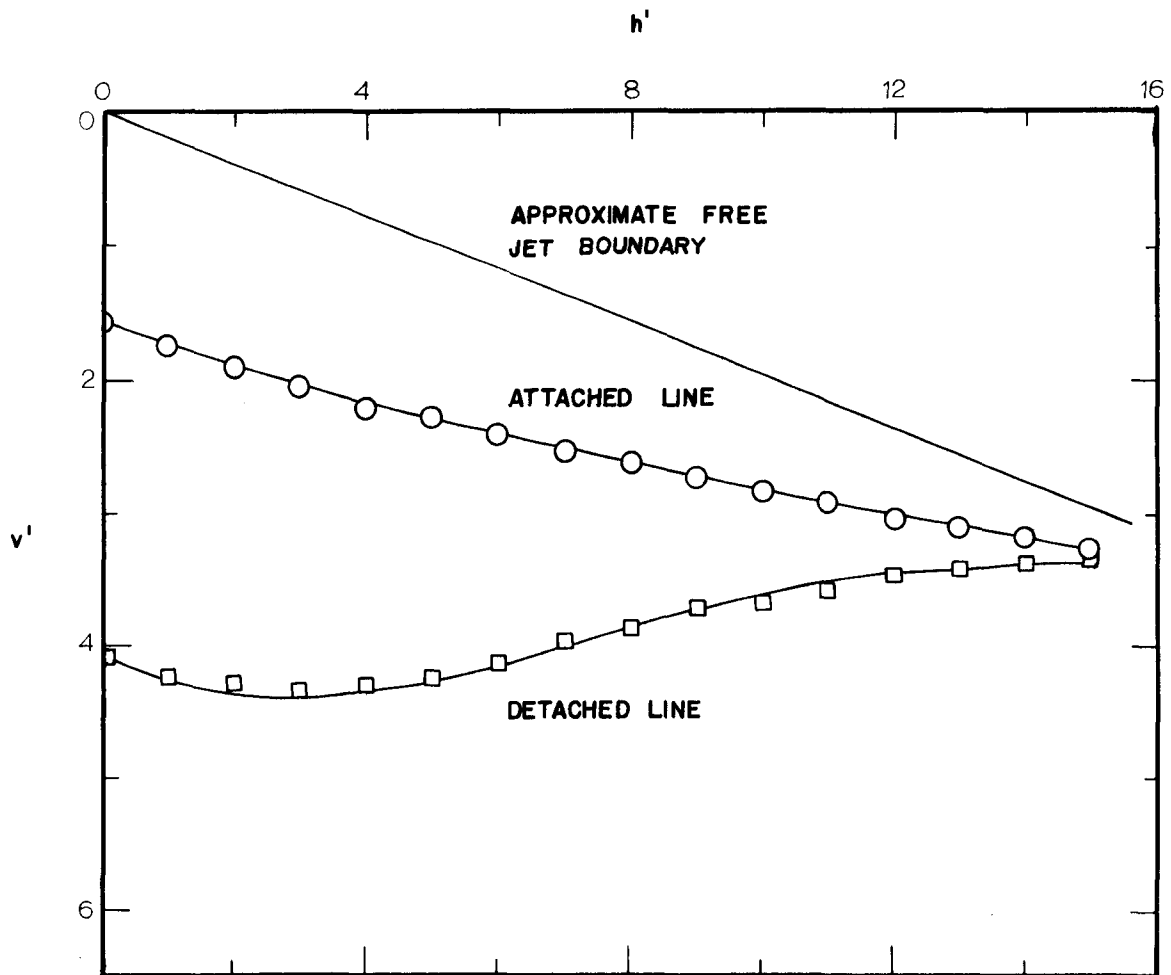
Fig. 4c HYSTERESIS PLOT (R = 3 in., t = 0.25 in.)

h'

Fig.4d HYSTERESIS PLOT (R=6 in., t=0.25 in)
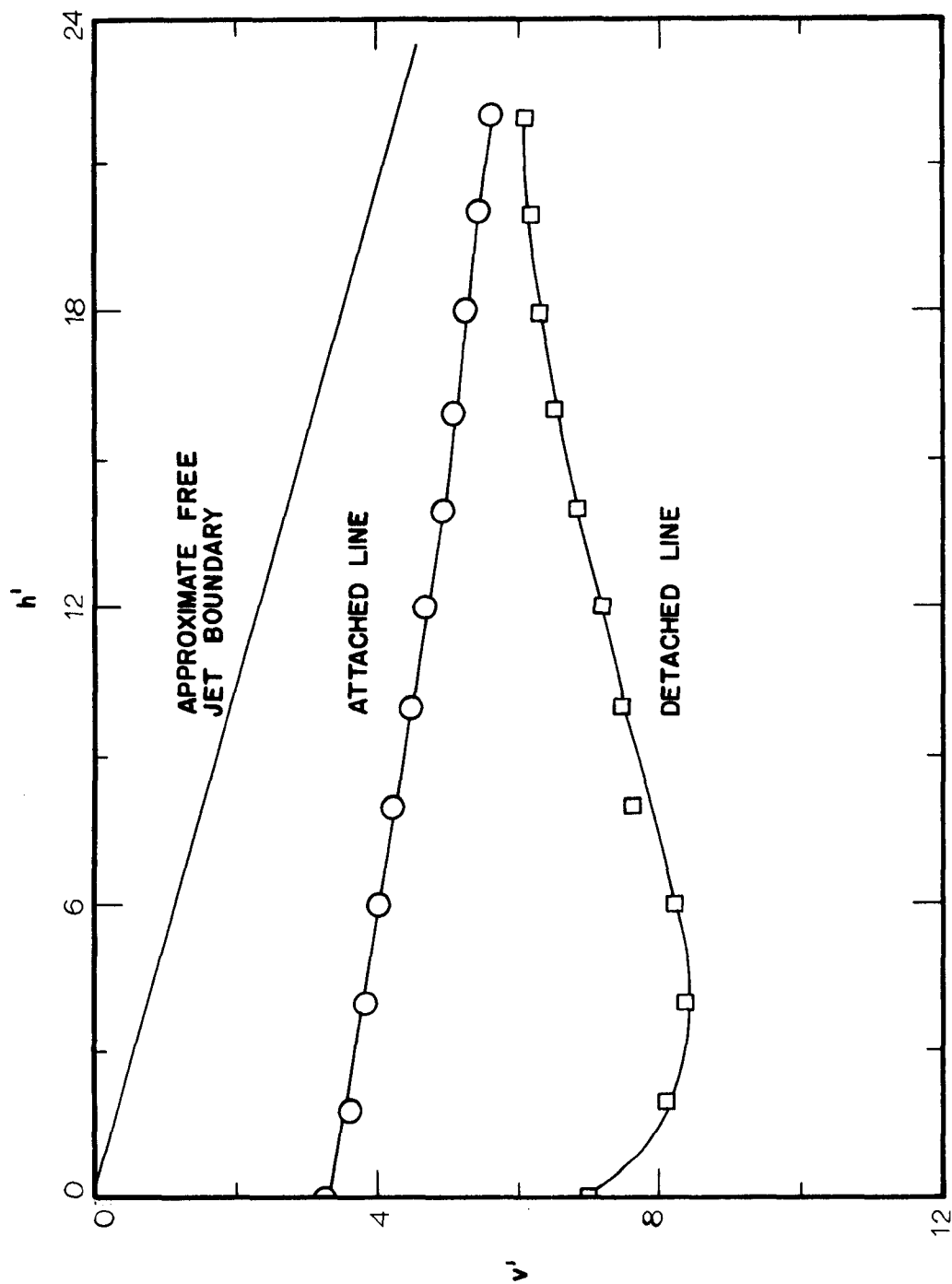
Fig. 4 e HYSTERESIS PLOT (R= 9 in., t = 0.25)

APPROXIMATE FREE
JET BOUNDARY

ATTACHED LINE

DETACHED LINE

h'

v'

Fig. 5 VISUALIZATION OF FLOW SEPARATION

LINE OF SEPARATION

JET
FLOW →
DIRECTION

SEPARATED
REGION

LEADING EDGE

TRAILING
EDGE
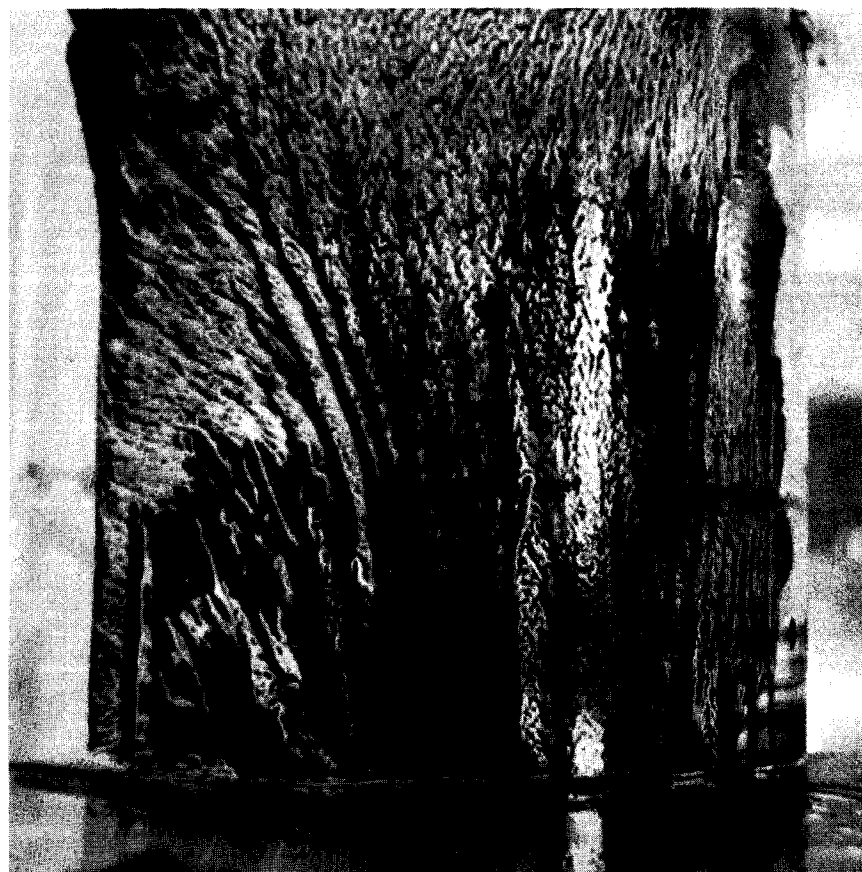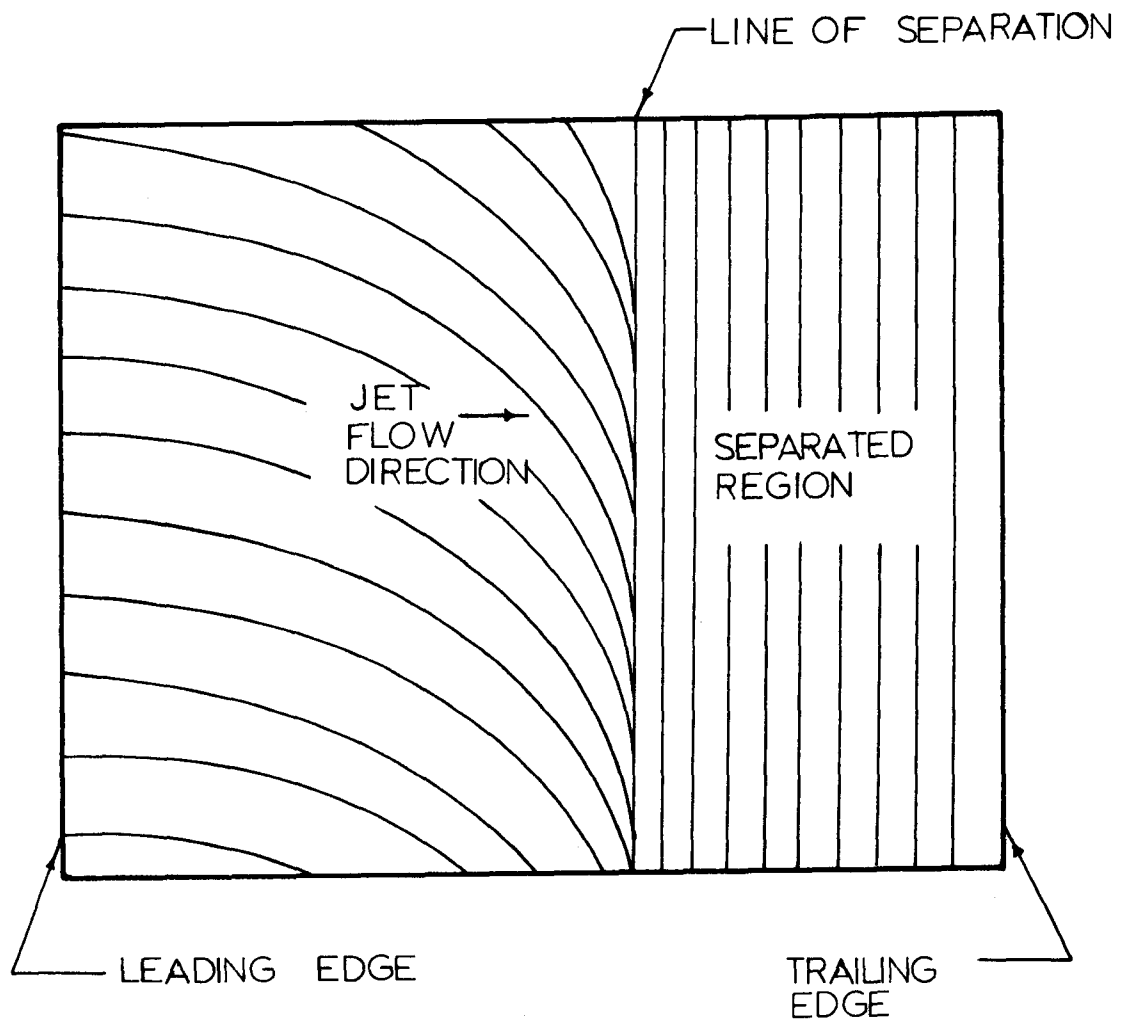
**Fig. 6 SKETCH OF LAMP BLACK TRACES
ON CURVED SURFACE**

Fig. 7 PLOT OF $h'_{max.}$VS. R'

3·0

2·4

$t=\frac{1}{16}$ in.

$t=\frac{1}{8}$ in.

$t=\frac{1}{4}$ in.

R = 9 in.

1·8

v_D (in)

1·2

h(in) = 1·5   1·0   0·5   0 $\frac{R}{(in)}$ $\frac{t}{(in)}$

R = 6 in.

				R (in)	t (in)
◐	◒	◑	○	3	$\frac{1}{4}$
◨	▣	◧	□	6	$\frac{1}{4}$
◈	◆	◈	◇	9	$\frac{1}{4}$
▲	▲	▲	△	3	$\frac{1}{8}$
◢	◣	◤	◁	6	$\frac{1}{8}$
◪	◩	◧	▷	9	$\frac{1}{8}$
◪	◨	◧	▷	3	$\frac{1}{16}$
◆	◆	◈	◇	6	$\frac{1}{16}$
◭	◮	◮	△	9	$\frac{1}{16}$

0·6

R = 3 in.

0

C   0·6   1·2   1·8   2·4
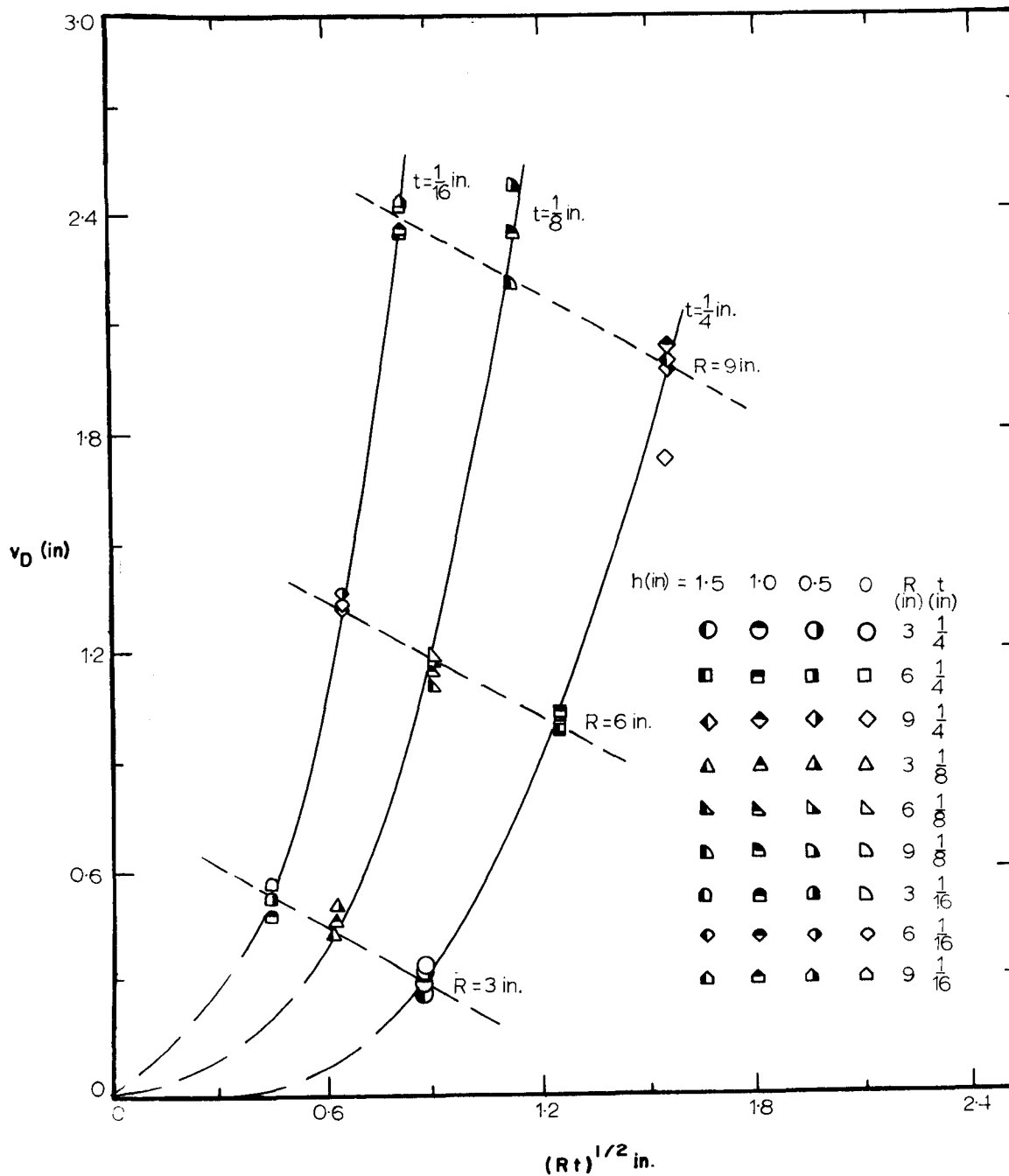
$(Rt)^{1/2}$ in.
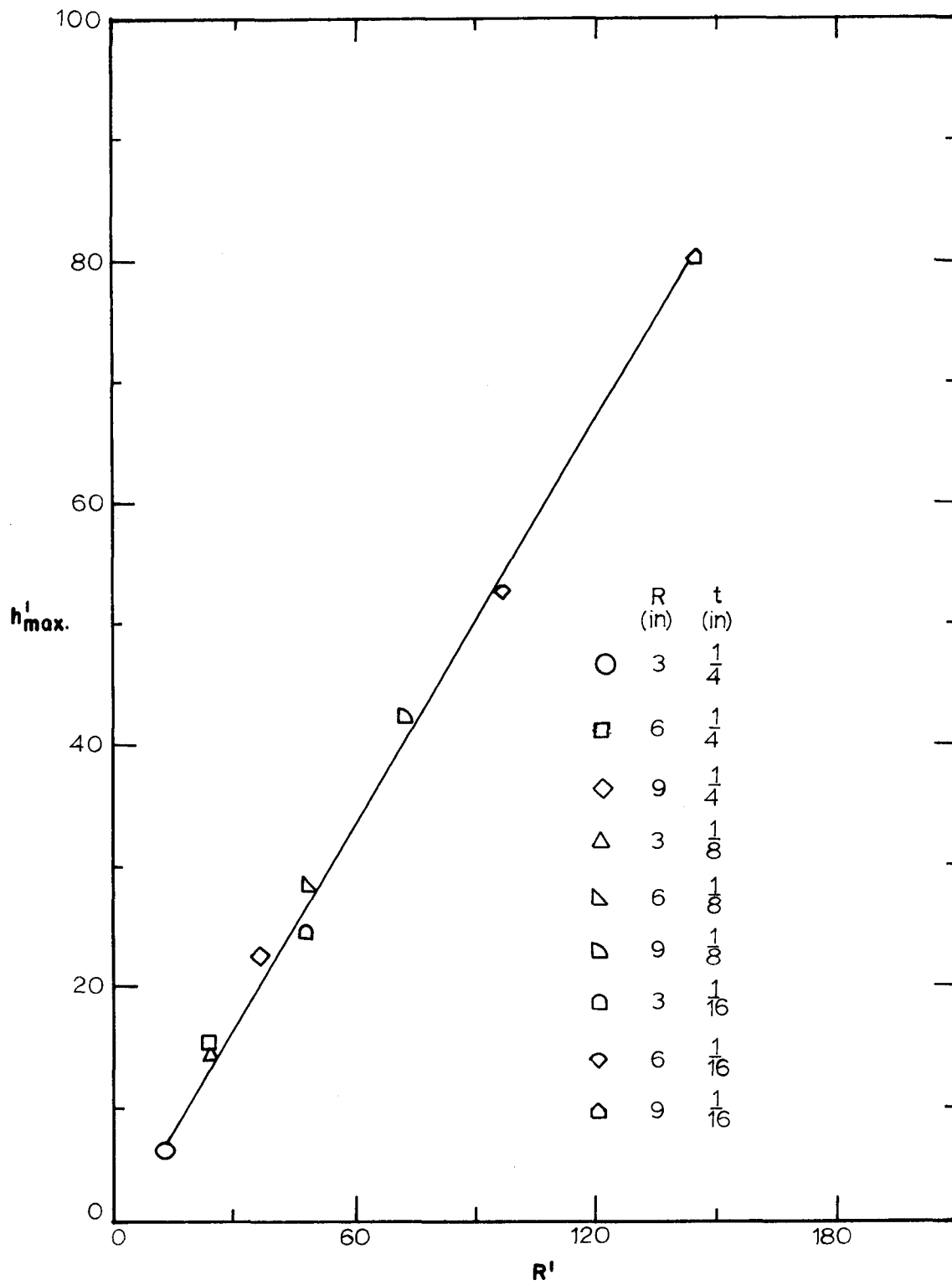
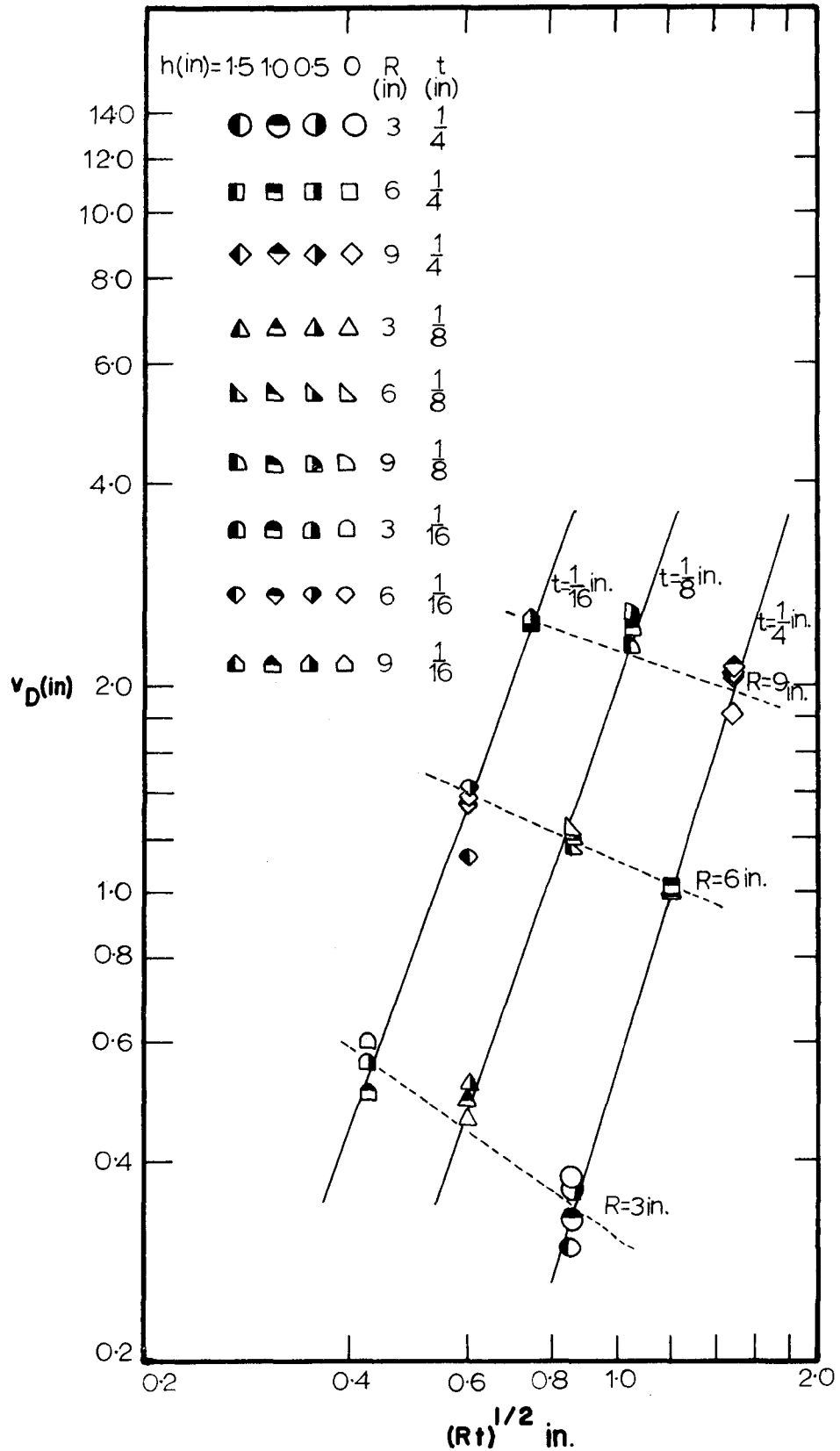Fig. 8 a DIMENSIONAL PLOT OF DETACHED POSITIONS
v_D VS. $(Rt)^{1/2}$

Fig. 8 b DIMENSIONAL PLOT OF DETACHED
POSITIONS v_D VS. $(Rt)^{1/2}$

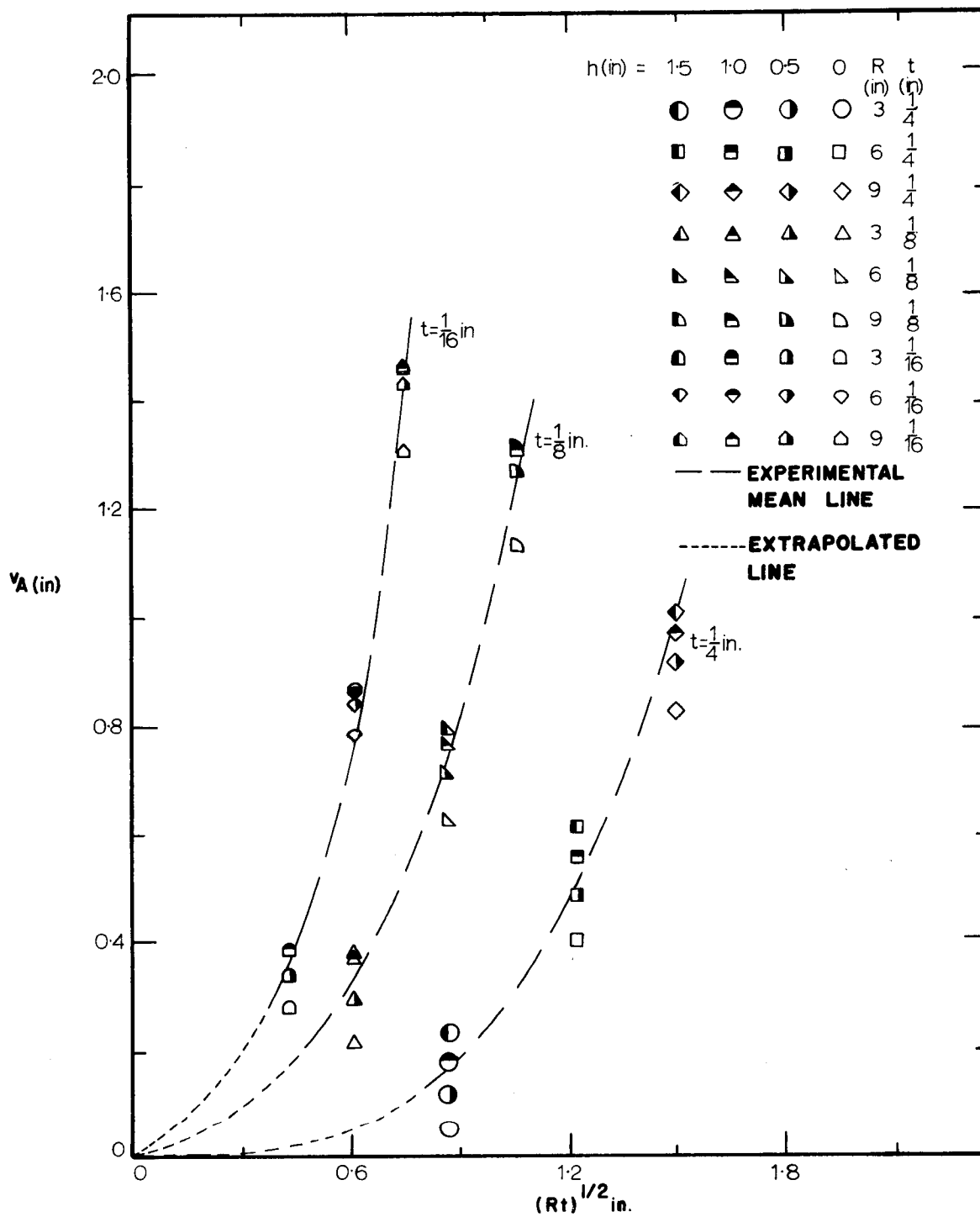Fig.9a DIMENSIONAL PLOT OF ATTACHED POSITIONS
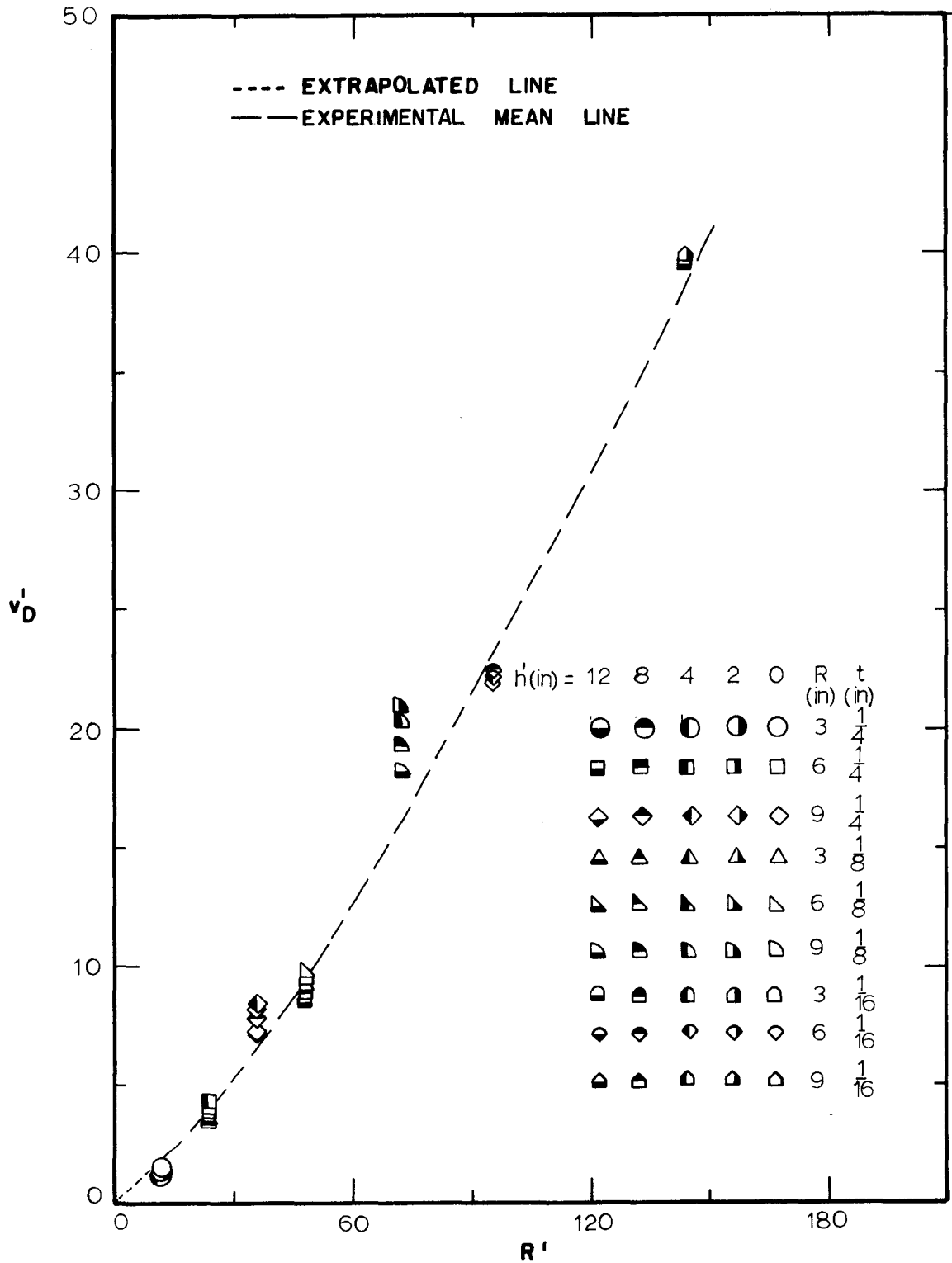
v_A VS. $(Rt)^{1/2}$

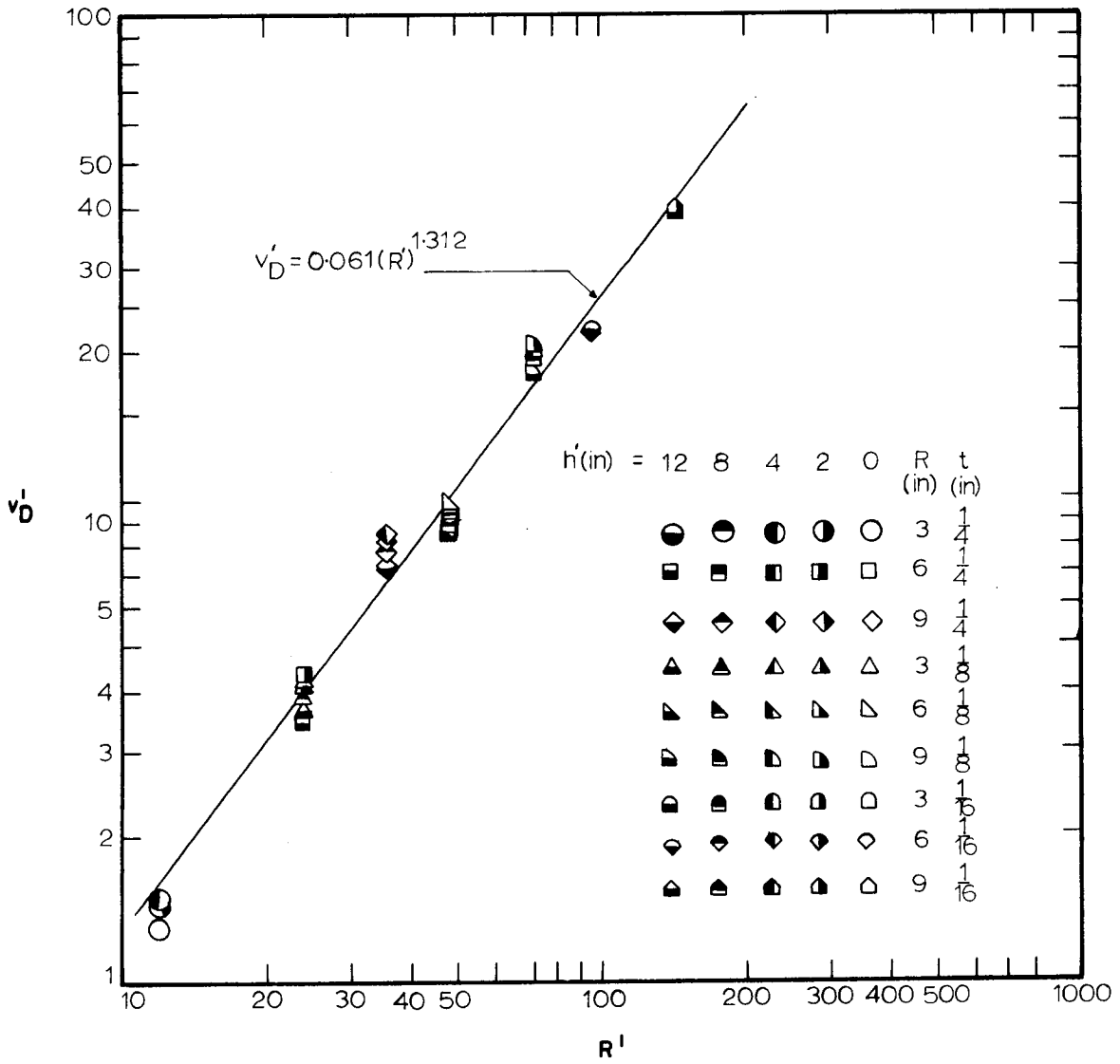Fig. 9 b DIMENSIONAL PLOT OF ATTACHED POSITIONS y_A VS. $(Rt)^{1/2}$

50

---- EXTRAPOLATED LINE
——EXPERIMENTAL MEAN LINE

40

30

v_D^I

20

h(in) = 12 8 4 2 0   R   t
                              (in) (in)
                          3   $\frac{1}{4}$
                          6   $\frac{1}{4}$
                          9   $\frac{1}{4}$
                          3   $\frac{1}{8}$
                          6   $\frac{1}{8}$
                          9   $\frac{1}{8}$
                          3   $\frac{1}{16}$
                          6   $\frac{1}{16}$
                          9   $\frac{1}{16}$

10

0

0   60   120   180

R'

Fig. 10a NON DIMENSIONAL PLOT OF DETACHED
POSITIONS (v_D^I VS. R')

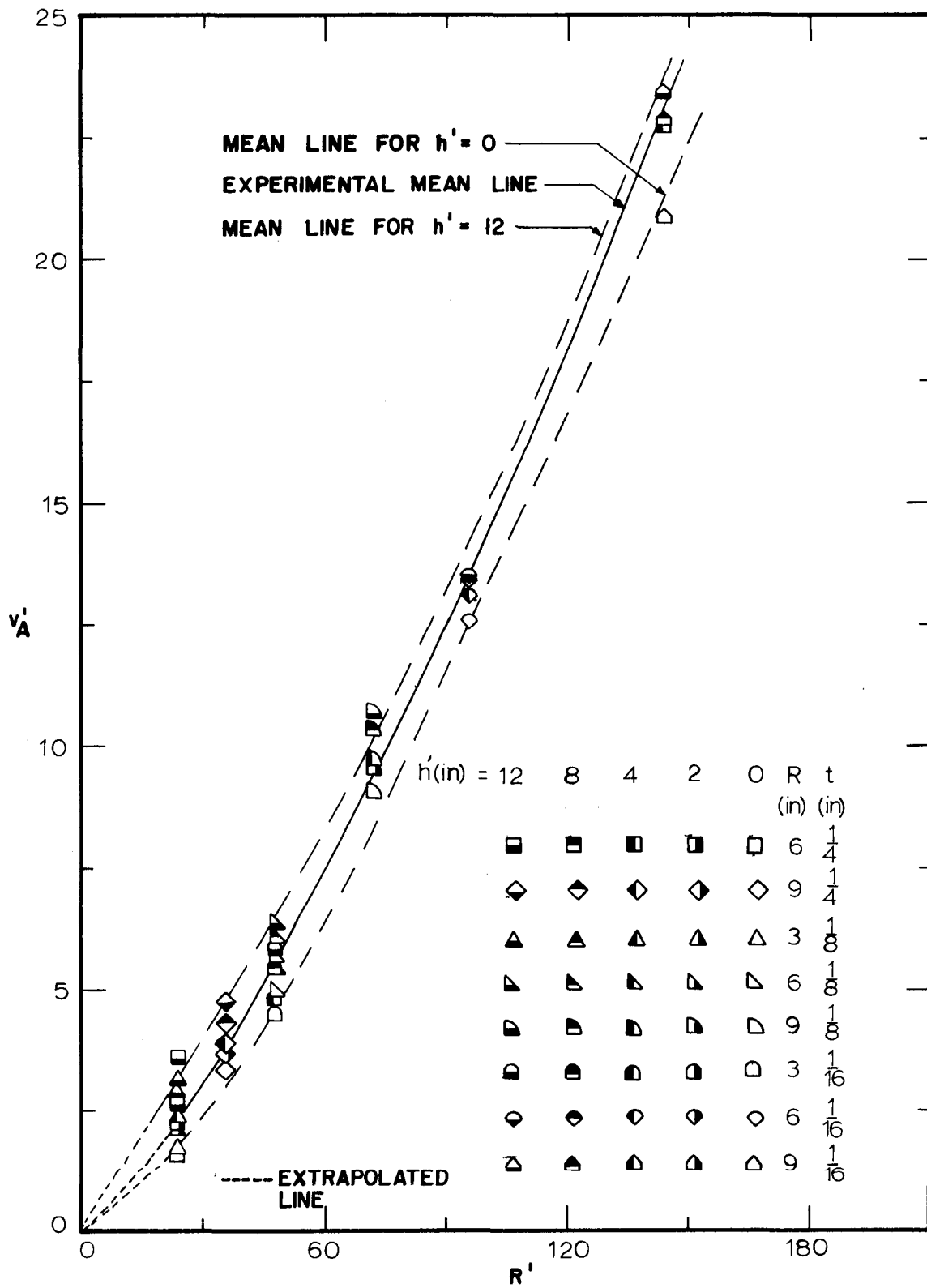Fig. 10 b   NON - DIMENSIONAL PLOT OF DETACHED POSITIONS

$(v'_D$ VS. $R')$

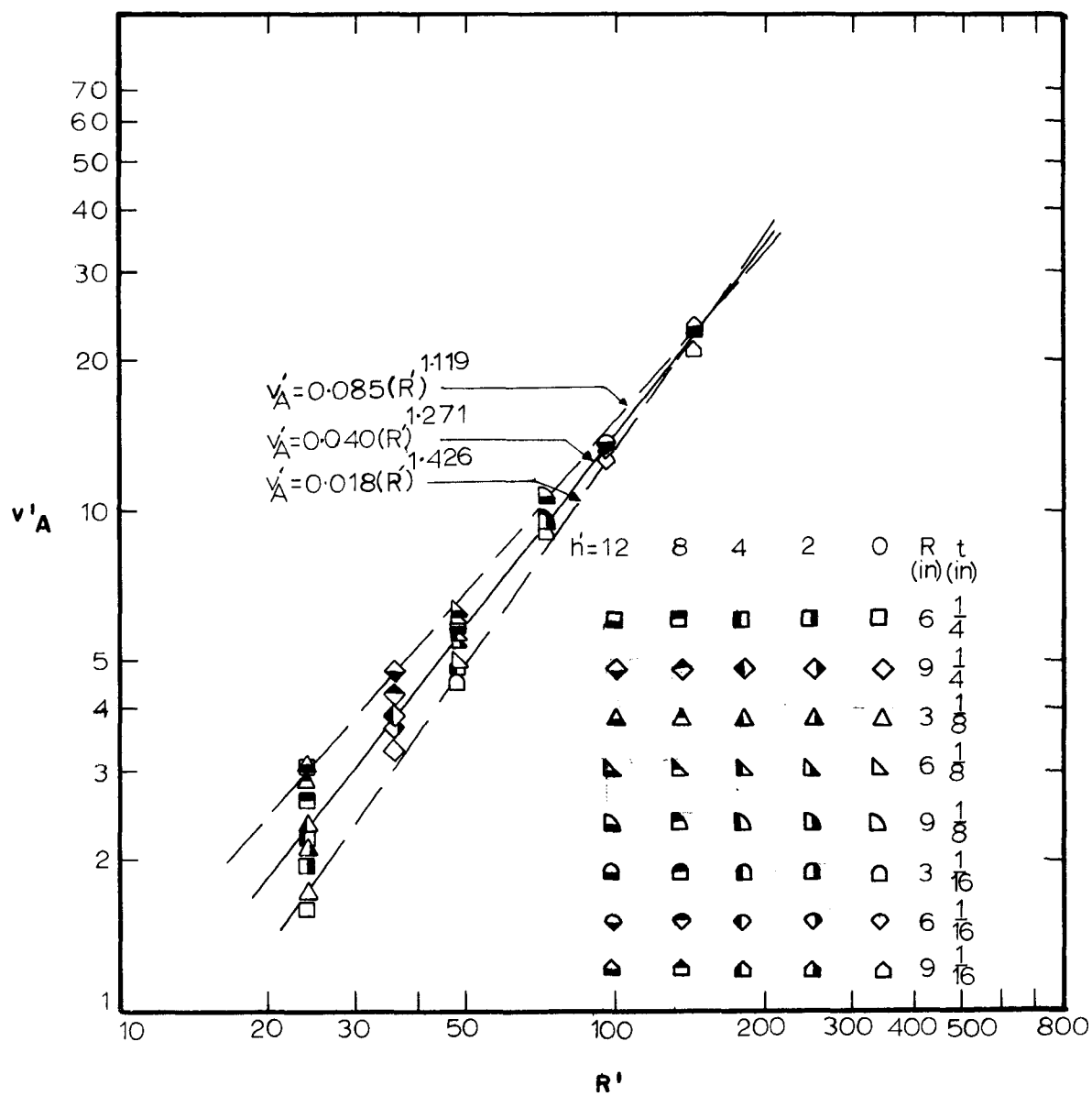FIG·IIa NON DIMENSIONAL PLOT OF ATTACHED POSITIONS

$(V_A' VS. R')$

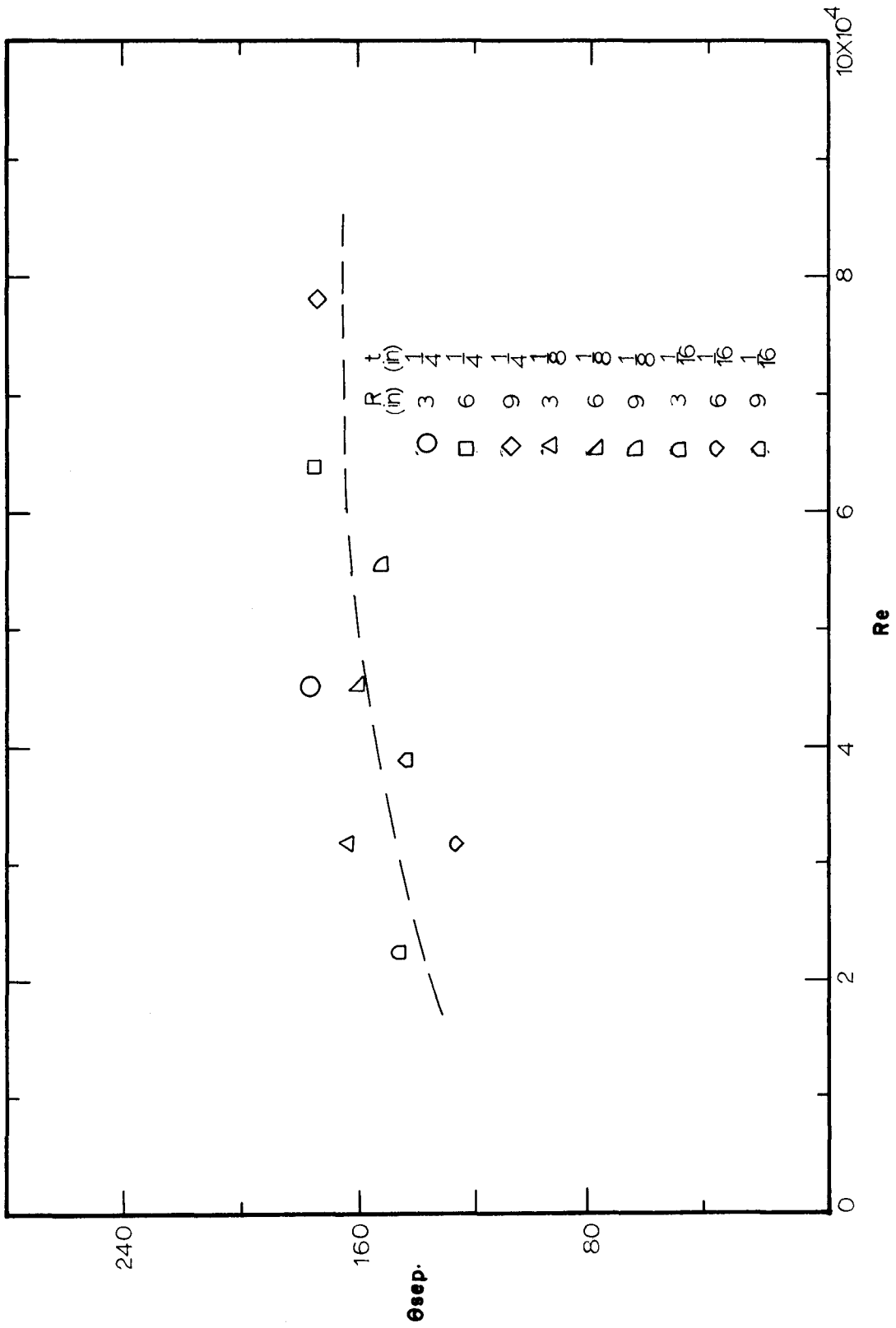Fig·IIb NON-DIMENSIONAL PLOT OF ATTACHED POSITIONS

$(v'_A$ VS·R')

Fig·12 VARIATION OF Θsep. WITH Re FOR NO GAP

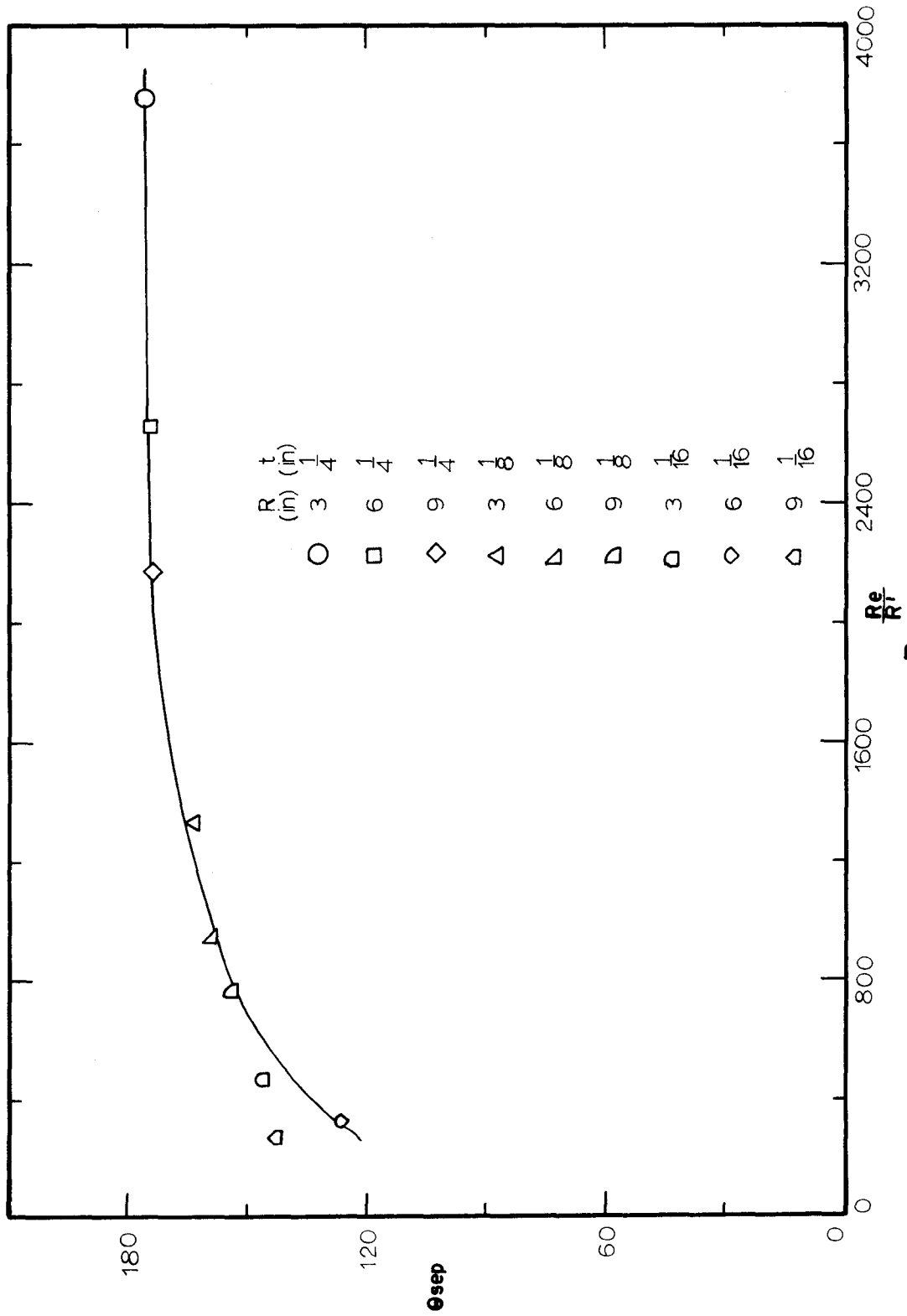Fig. 13 VARIATION OF θsep. WITH $\frac{Re}{R_i}$ FOR FOR NO GAP

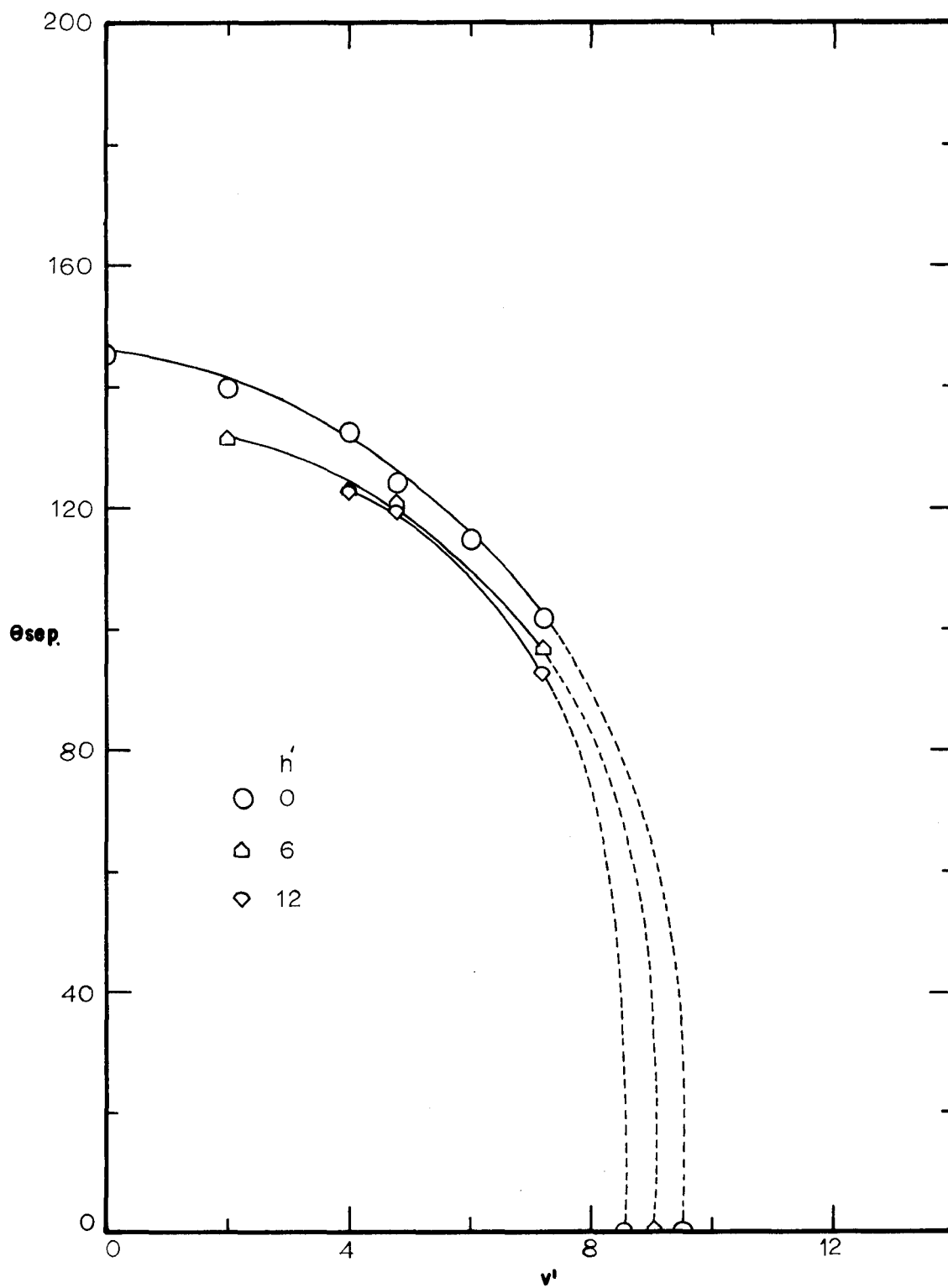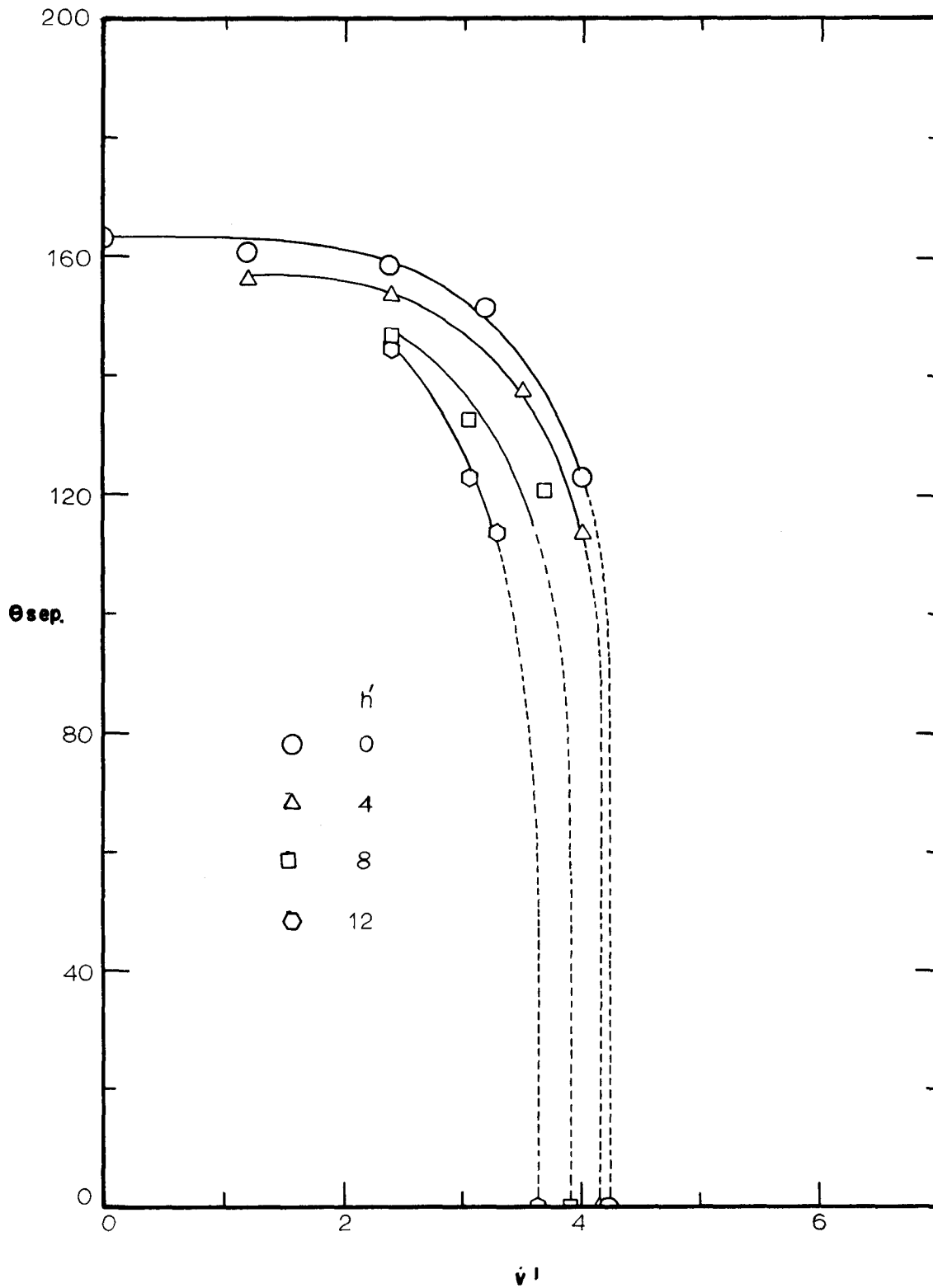Fig. 14a PLOTS OF Θsep. VS. v' FOR DIFFERENT h'
(R = 3 in., t = 0.0625 in)

Fig.I4b PLOTS OF θsep. VS. v' FOR DIFFERENT h'
(R=3 in., t=0.125 in.)

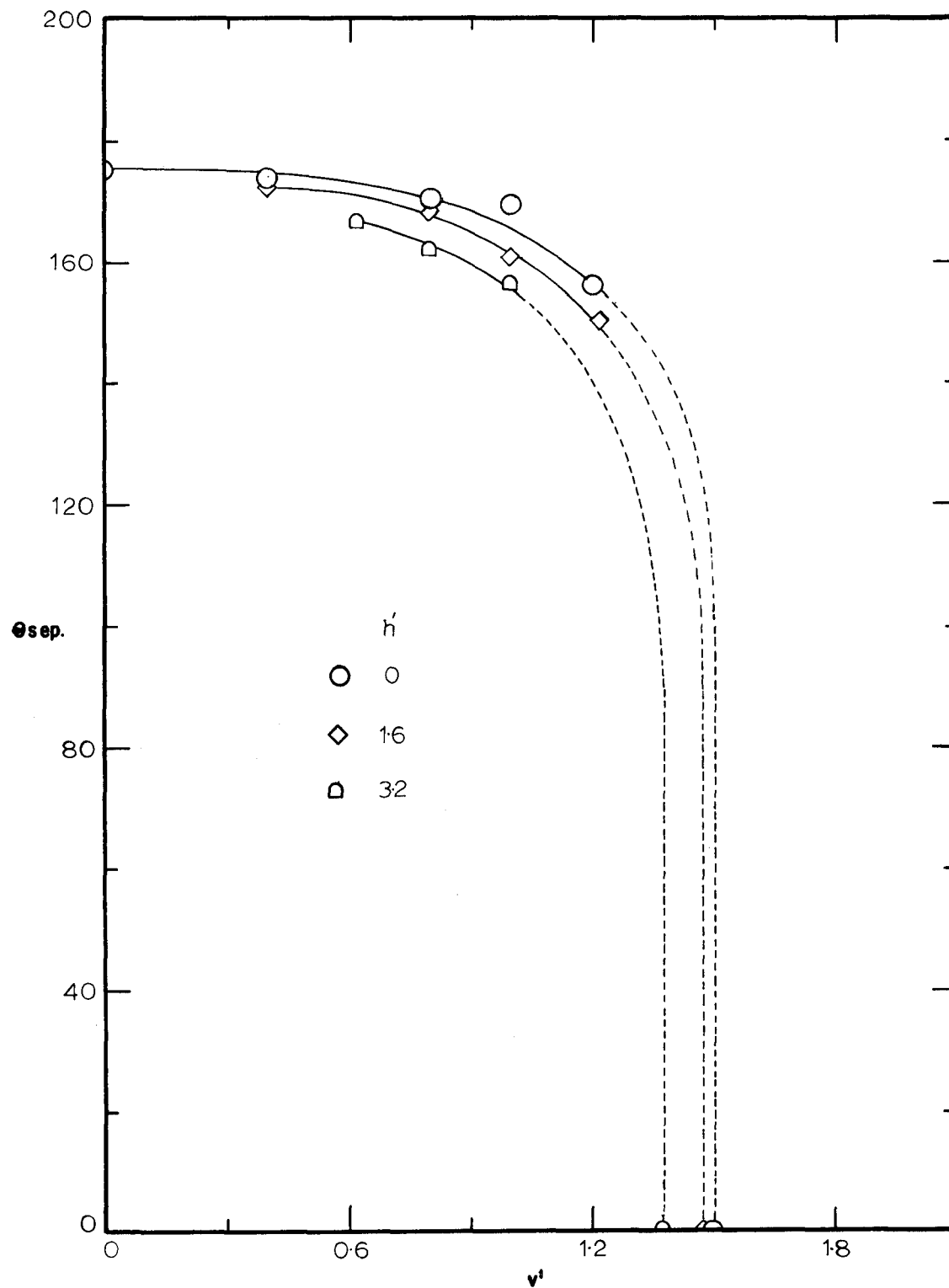Fig. 14 c   PLOT OF Θsep. VS. V' FOR DIFFERENT h'
(R = 3 in., t = 0.25 in)

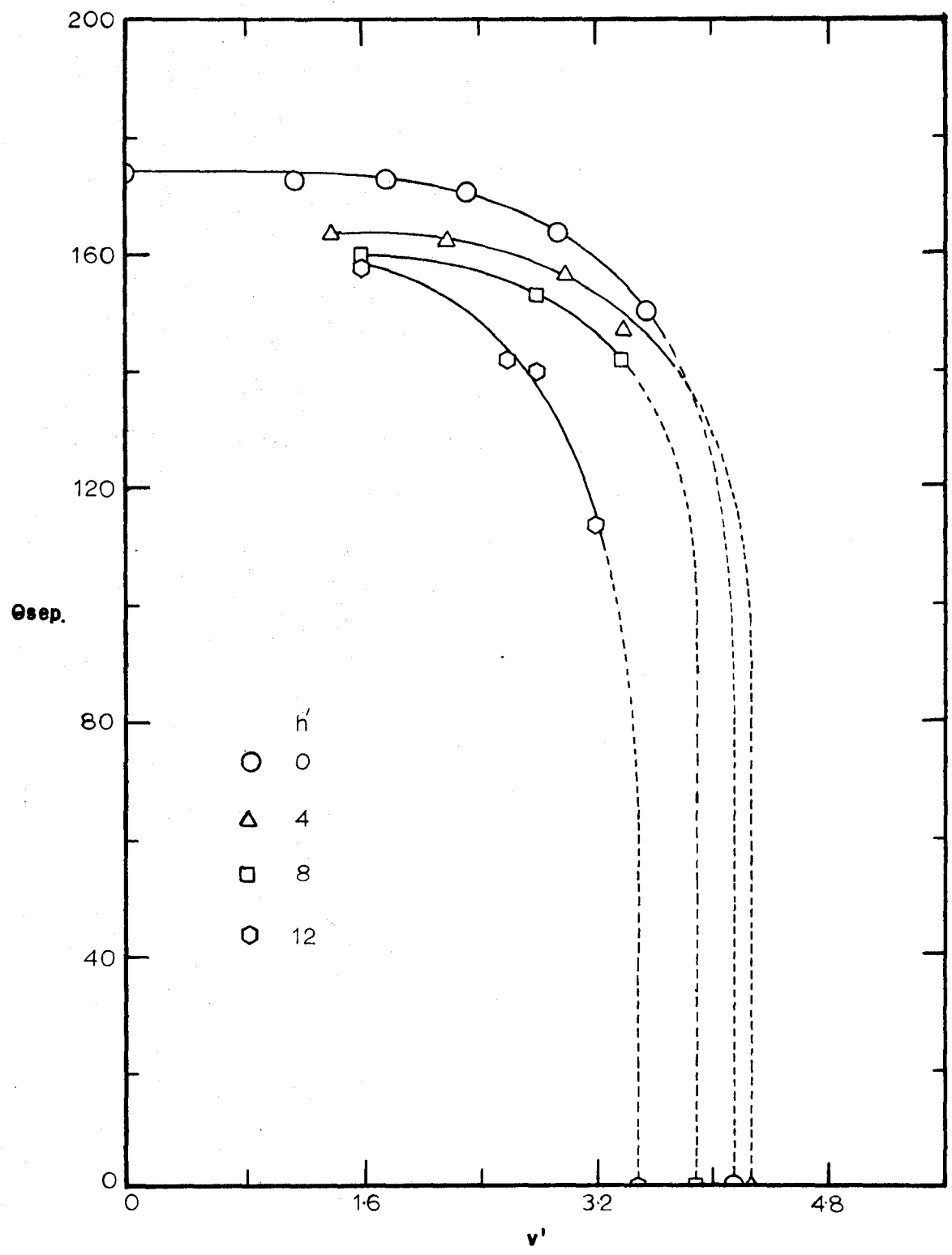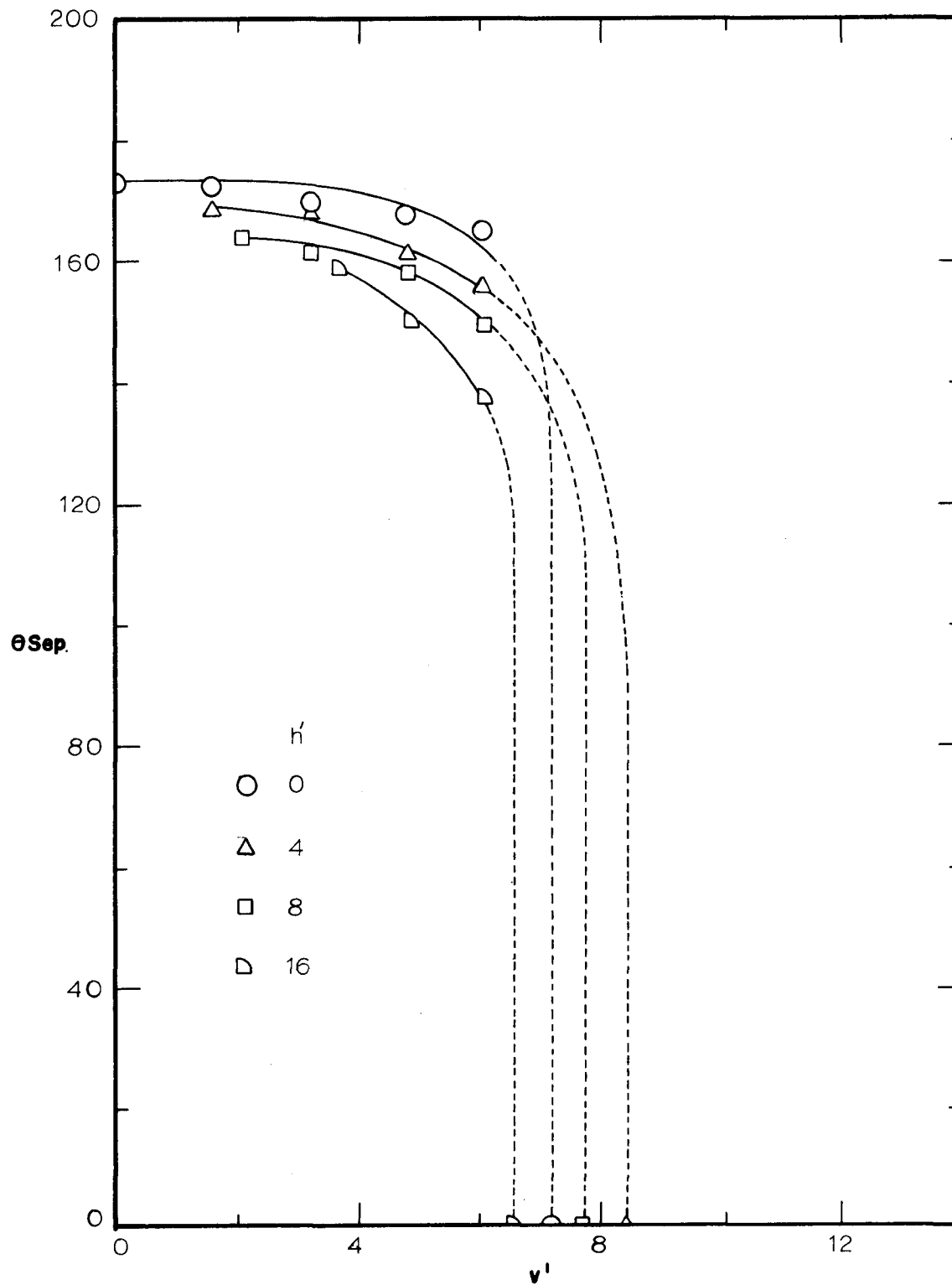Fig. l4d PLOT OF Θsep. VS. v' FOR DIFFERENT h'
(R=6 in., t= 0.25 in)

Fig. 14 e PLOTS OF θ sep. VS. v' FOR DIFFERENT h'
(R =.9 in ., t=0.25 in)

Fig.15a PLOT OF Θsep. VS. $\frac{Re}{R'}$ FOR DIFFERENT $\frac{v}{v_D}$

$\frac{v}{v_D} = 0.6$

R (in)	t (in)	
○	3	$\frac{1}{4}$
□	6	$\frac{1}{4}$
◇	9	$\frac{1}{4}$
◁	3	$\frac{1}{8}$
△	6	$\frac{1}{8}$
◁	3	$\frac{1}{16}$
◇	6	$\frac{1}{16}$
◁	9	$\frac{1}{16}$

180

120

60

Θsep.

0   800   1600   2400   3200   4000
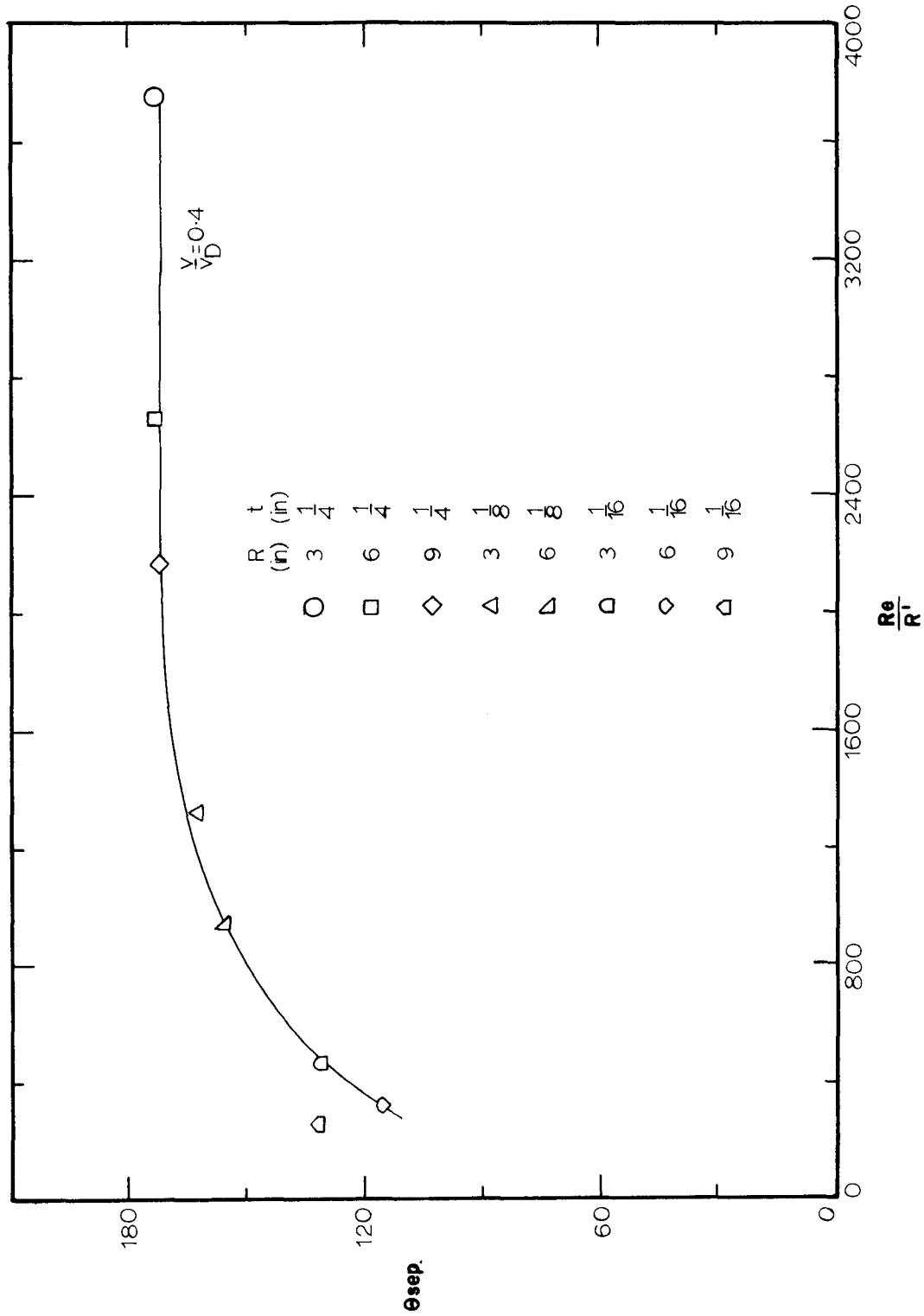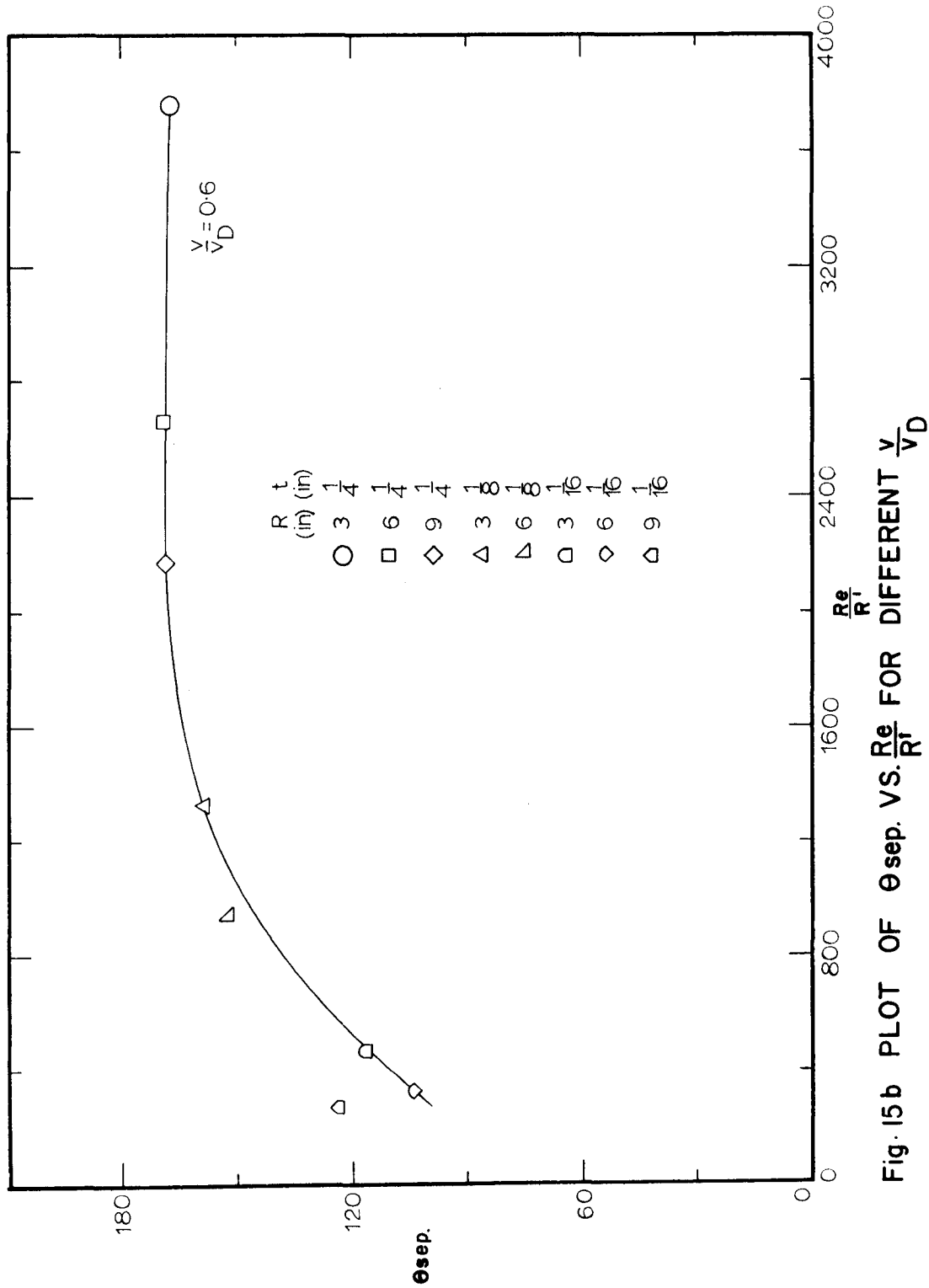
$\frac{Re}{R^1}$

Fig. 15 b PLOT OF Θsep. VS. $\frac{Re}{R^1}$ FOR DIFFERENT $\frac{v}{v_D}$

$$\frac{v}{v_D} = 0.8$$

R (in)	t (in)	
○	3	$\frac{1}{4}$
□	6	$\frac{1}{4}$
◇	9	$\frac{1}{4}$
◁	3	$\frac{1}{8}$
△	6	$\frac{1}{8}$
◁	3	$\frac{1}{16}$
◇	6	$\frac{1}{16}$
◁	9	$\frac{1}{16}$

Θsep.

180

120

60

0

0   800   1600   2400   3200   4000

$\frac{Re}{R'}$
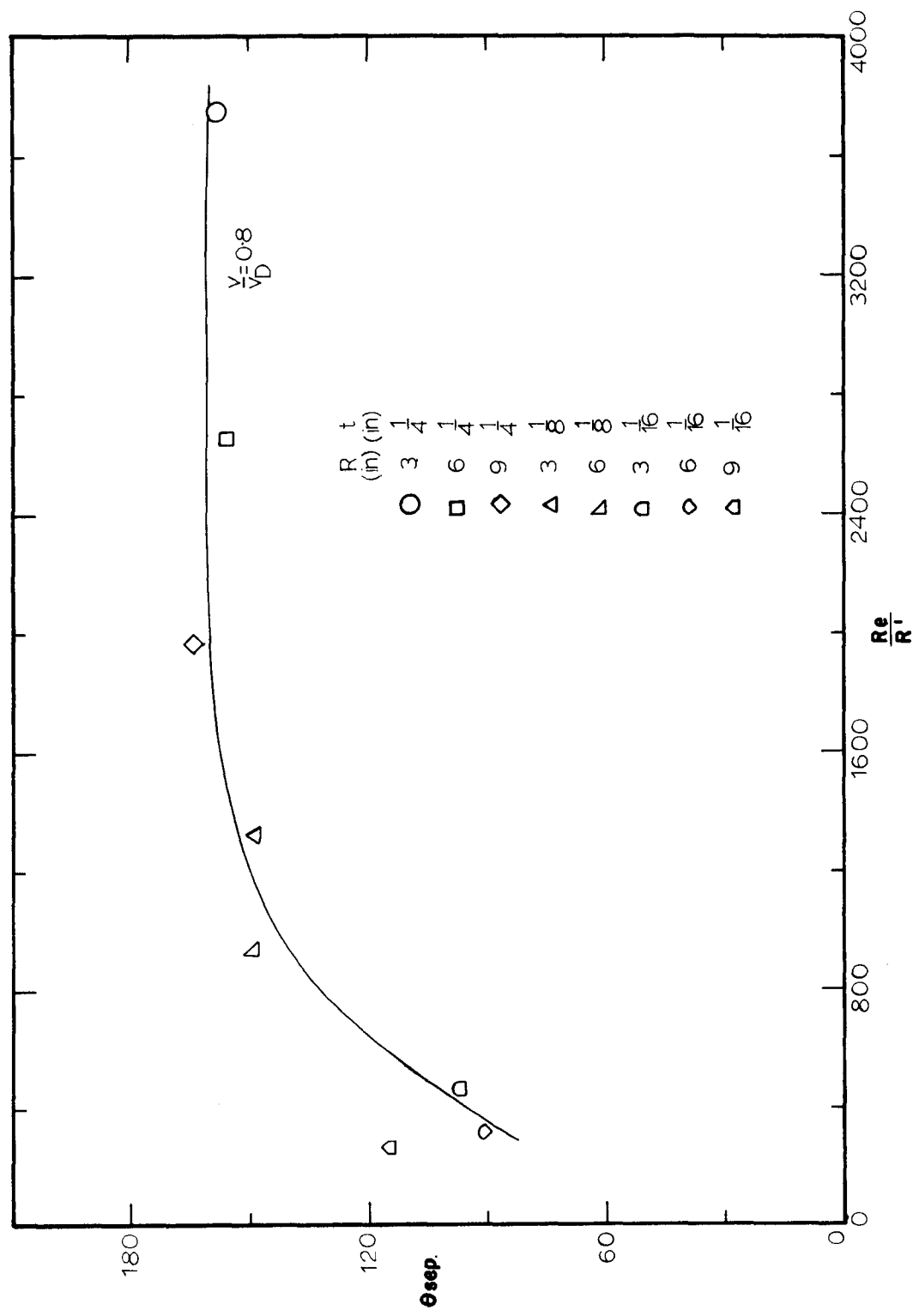
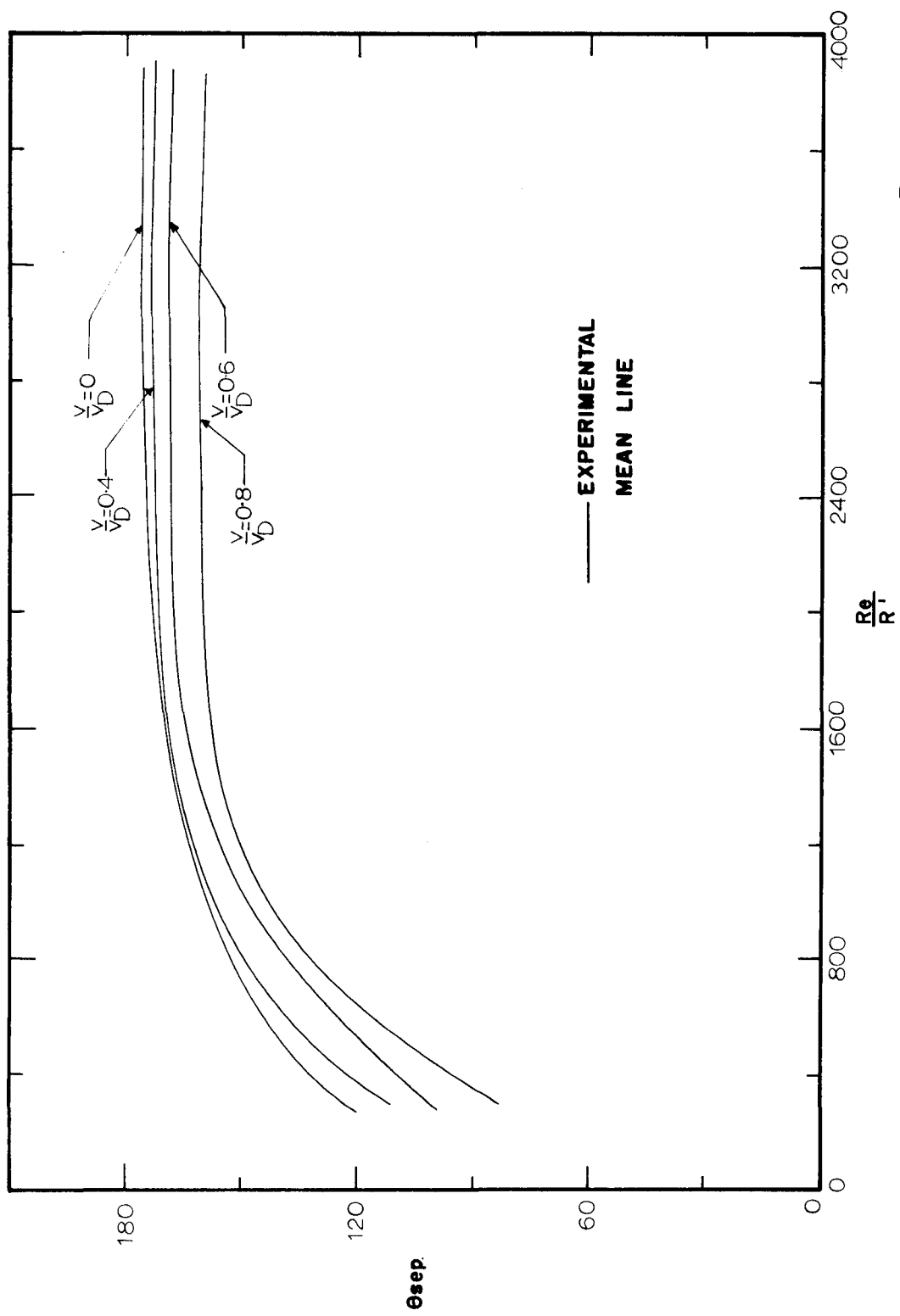Fig. 15c PLOT OF Θsep. VS $\frac{Re}{R'}$ FOR DIFFERENT $\frac{v}{v_D}$

Fig. 16 EXPERIMENTAL MEAN LINES FOR DIFFERENT $\frac{v}{v_D}$ (Θsep vs. $\frac{Re}{R'}$)

APPENDIX

DIMENSIONAL ANALYSIS

For the present investigation, it is assumed that the following relation is true:

$$\Theta_{Sep.} = f\left[(P_T-P_a),\rho,\nu,t,R,h,v\right]$$

In the M,L,T system of units, the dimensional matrix for the parameters is:

	1	2	3	4	5	6	7	8
	$\Theta_{Sep.}$ ν	R	h	v	(P_T-P_a)	ρ	t
M	0	0	0	0	0	1	1	0
L	0	2	1	1	1	-1	-3	1
T	0	-1	0	0	0	-2	0	0

It is apparent that the rank (r) of the matrix is three (3) and since there are eight (8) variables, the number of dimensionless groups is 8-3 = 5.

Taking (P_T-P_a), ρ and t as the repeating variables, the dimensionless groups can be expressed as:

$$\Pi_1 = \Theta_{Sep.}$$
$$\Pi_2 = (P_T-P_a)^{x_1} (\rho)^{y_1} (t)^{z_1} \nu$$
$$\Pi_3 = (P_T-P_a)^{x_2} (\rho)^{y_2} (t)^{z_2} R$$
$$\Pi_4 = (P_T-P_a)^{x_3} (\rho)^{y_3} (t)^{z_2} h$$
$$\Pi_5 = (P_T-P_a)^{x_4} (\rho)^{y_4} (t)^{z_4} v$$

Further the dimensionless groups are:

$$\Pi_1 = \Theta_{Sep.}$$

$$\Pi_2 = \left[\frac{(P_T - P_a) t^2}{\rho \, v^2} \right]^{-\frac{1}{2}}$$

$$\Pi_3 = \frac{R}{t}$$

$$\Pi_4 = \frac{h}{t}$$

$$\Pi_5 = \frac{v}{t}$$

Dividing Π_2 by $(\Pi_3)^{\frac{1}{2}}$, we get the dimensionless group as:

$$\Pi_6 = \frac{\Pi_2}{(\Pi_3)^{\frac{1}{2}}}$$

$$= \left[\frac{(P_T - P_a) R t}{\rho \, v^2} \right]^{-\frac{1}{2}}$$

Hence the relationship can be written as:

$$F \left[\Theta_{Sep.}, \left\{ \frac{(P_T - P_a) R t}{\rho \, v^2} \right\}^{-\frac{1}{2}}, \frac{R}{t}, \frac{h}{t}, \frac{v}{t} \right] = 0$$

VITA AUCTORIS

1938   Born at Admabad, India on August 20.

1955   Completed high school education at Model High School, Jabalpur, India.

1957   Completed Intermediate Science Course at Mahakoshal Mahavidyalaya, Jabalpur, India.

1961   Received the Degree of Bachelor of Engineering (Honours) in Mechanical Engineering from Government Engineering College, Jabalpur, India.

1962   Finished the course requirements for Master of Engineering Degree in Mechanical Engineering at Roorkee University, Roorkee, India. Joined the engineering staff of M/S Heavy Engineering Corporation Ltd., Ranchi, India.

1964   Received the Degree of Master of Engineering in Mechanical Engineering at Roorkee University, Roorkee, India.

1967   Currently a candidate for the Degree of Master of Applied Science in Mechanical Engineering at the University of Windsor.